The Light company Houston Lighting & Power P.O. Box 1700 Houston, Texas 77001 (713) 228-9211

October 22, 1985
ST-HL-AE-1432
File No.: G9.17

Mr. George W. Knighton, Chief
Licensing Branch No. 3
Division of Licensing
U. S. Nuclear Regulatory Commission
Washington, DC 20555

South Texas Project
Units 1 and 2
Docket Nos. STN 50-498, STN 50-499
Responses to DSER/FSAR Items
Update of Table 4.3-1, Construction Materials

Dear Mr. Knighton:

The attachments enclosed provide STP's response to Draft Safety Evaluation Report (DSER) or Final Safety Analysis Report (FSAR) items.

The item numbers listed below correspond to those assigned on STP's internal list of items for completion which includes open and confirmatory DSER items, STP FSAR open items and open NRC questions. This list was given to your Mr. N. Prasad Kadambi on October 8, 1985 by our Mr. M. E. Powell.

The attachments include mark-ups of FSAR pages which will be incorporated in a future FSAR amendment unless otherwise noted below.

The items which are attached to this letter are:

Attachment	Item No.*	Subject
1	F 4.3-1	Update of Table 4.3-1, Construction Materials. Note: This attachment also includes a general update of Chapter 4.

* Legend
D - DSER Open Item C - DSER Confirmatory Item
F - FSAR Open Item Q - FSAR Question Response Item

Bool
1/1

L1/DSER/ao

If you should have any questions concerning this matter, please contact Mr. Powell at (713) 993-1328.

Very truly yours,

M. R. Wisenburg
Manager, Nuclear Licensing

JSP/bl

Attachments: See above

L1/DSER/ao

cc:

Hugh L. Thompson, Jr., Director
Division of Licensing
Office of Nuclear Reactor Regulation
U.S. Nuclear Regulatory Commission
Washington, DC 20555

Robert D. Martin
Regional Administrator, Region IV
Nuclear Regulatory Commission
611 Ryan Plaza Drive, Suite 1000
Arlington, TX 76011

N. Prasad Kadambi, Project Manager
U.S. Nuclear Regulatory Commission
7920 Norfolk Avenue
Bethesda, MD 20814

Claude E. Johnson
Senior Resident Inspector/STP
c/o U.S. Nuclear Regulatory Commission
P.O. Box 910
Bay City, TX 77414

M.D. Schwarz, Jr., Esquire
Baker & Botts
One Shell Plaza
Houston, TX 77002

J.R. Newman, Esquire
Newman & Holtzinger, P.C.
1615 L Street, N.W.
Washington, DC 20036

Director, Office of Inspection and Enforcement
U.S. Nuclear Regulatory Commission
Washington, DC 20555

E.R. Brooks/R.L. Range
Central Power & Light Company
P.O. Box 2121
Corpus Christi, TX 78403

H.L. Peterson/G. Pokorny
City of Austin
P.O. Box 1088
Austin, TX 78767

J.B. Poston/A. vonRosenberg
City Public Service Board
P.O. Box 1771
San Antonio, TX 78296

Brian E. Berwick, Esquire
Assistant Attorney General for the State of Texas
P.O. Box 12548, Capitol Station
Austin, TX 78711

Lanny A. Sinkin
3022 Porter Street, N.W. #304
Washington, DC 20008

Oreste R. Pirfo, Esquire
Hearing Attorney
Office of the Executive Legal Director
U.S. Nuclear Regulatory Commission
Washington, DC 20555

Charles Bechhoefer, Esquire
Chairman, Atomic Safety & Licensing Board
U.S. Nuclear Regulatory Commission
Washington, DC 20555

Dr. James C. Lamb, III
313 Woodhaven Road
Chapel Hill, NC 27514

Judge Frederick J. Shon
Atomic Safety and Licensing Board
U.S. Nuclear Regulatory Commission
Washington, DC 20555

Mr. Ray Goldstein, Esquire
1001 Vaughn Building
807 Brazos
Austin, TX 78701

Citizens for Equitable Utilities, Inc.
c/o Ms. Peggy Buchorn
Route 1, Box 1684
Brazoria, TX 77422

Docketing & Service Section
Office of the Secretary
U.S. Nuclear Regulatory Commission
Washington, DC 20555
(3 Copies)

Advisory Committee on Reactor Safeguards
U.S. Nuclear Regulatory Commission
1717 H Street
Washington, DC 20555

Revised 9/25/85

L1/DSER/ao

TABLE 4.1-1 (Continued)

REACTOR DESIGN COMPARISION TABLE

CORE MECHANICAL DESIGN PARAMETERS	W. B. McGuire UNITS 1 & 2	South Texas Project UNITS 1 & 2
26. Design	RCC Canless 17 x 17	RCC Canless 17 x 17
27. Number of Fuel Assemblies	193	193
28. UO_2 Rods per Assembly	264	264
29. Rod Pitch, in.	0.496	0.496
30. Overall Dimensions, in.	8.426 x 8.426	8.426 x 8.426
31. Fuel Weight (as UO_2), lb	222,739	~~259,860~~ 261,000 (Nominal)
32. Zircalloy Weight, lb	50,913	54,840
33. Number of Grids per Assembly	8 - Type R	10 - Type R
34. Loading Technique	3 region non-uniform	3 region non-uniform

18

ATTACHMENT 1
ST-HL-AE-1432
PAGE 1 OF 54

TABLE 4.1-2 (Continued)

ANALYTICAL TECHNIQUES IN CORE DESIGN

Analysis	Technique	Computer Code	Section Referenced
Nuclear Design (Continued)			
	Group constants for control rods with self-shielding	HAMMER-AIM	4.3.3.2
2. X-Y Power Distributions, Fuel Depletion, Critical Boron Concentrations, x-y Xenon Distributions, Reactivity Coefficients	2-D, 2-Group Diffusion Theory	TURTLE	4.3.3.3
	2-D and 3-D Diffusion Theory-based Nodal Method	PALADON	4.3.3.3
3. Axial Power Distributions, Control Rod Worths, and Axial Xenon Distribution	1-D, 2-Group Diffusion Theory	PANDA	4.3.3.3
4. Fuel Rod Power	Integral Transport Theory	LASER	4.3.3.1
Effective Resonance Temperature	Monte Carlo Weighting Function	REPAD	

ATTACHMENT 1
ST-HL-AE-1432
PAGE 2 OF 54

4.2 FUEL SYSTEM DESIGN

The plant conditions for design are divided into four categories in accordance with their anticipated frequency of occurrence and risk to the public: Condition I - Normal Operation; Condition II - Incidents of Moderate Frequency; Condition III - Infrequent Incidents; Condition IV - Limiting Faults. The bases and description of plant operation and events involving each Condition are given in the Accident Analysis Chapter 15.

The reactor is designed so that its components meet the following performance and safety criteria:

1. The mechanical design of the reactor core components and their physical arrangement, together with corrective actions of the reactor control, protection and emergency cooling systems (when applicable) assure that:

   a. Fuel damage* is not expected during Condition I and Condition II events. It is not possible, however, to preclude a very small number of rod failures. These are within the capability of the plant cleanup system and are consistent with plant design bases.

   b. The reactor can be brought to a safe state following a Condition III event with only a small fraction of fuel rods damaged* although sufficient fuel damage might occur to preclude immediate resumption of operation.

   c. The reactor can be brought to a safe state and the core can be kept subcritical with acceptable heat transfer geometry following transients arising from Condition IV events.

2. The fuel assemblies are designed to withstand, without exceeding the criteria of Section 4.2.1.5, loads induced during shipping, handling and core loading.

3. The fuel assemblies are designed to accept control rod insertions in order to provide the required reactivity control for power operations and reactivity shutdown conditions.

4. All fuel assemblies have provisions for the insertion of incore instrumentation necessary for plant operation.

5. The reactor internals in conjunction with the fuel assemblies and incore control components direct reactor coolant through the core. This achieves acceptable flow distribution and restricts bypass flow so that the heat transfer performance requirements can be met for all modes of operation.

*Fuel damage as used here is defined as penetration of the fission product barrier (i.e., the fuel rod cladding).

the clad has some capability for accommodating plastic strain, the yield stress has been accepted as a conservative design basis.

2) Clad Tensile Strain

from the unirradiated condition. The elastic tensile strain during a transient is less than 1% from the pretransient value.

total tensile creep

The strain is less than one percent. This limit is consistent with proven practice.

c. Vibration and Fatigue

1) Strain Fatigue

The cumulative strain fatigue cycles are less than the design strain fatigue life. This basis is consistent with proven practice.

2) Vibration

Potential fretting wear due to vibration is prevented assuring that the stress-strain limits are not exceeded during design life. Fretting of the clad surface can occur due to flow-induced vibration between the fuel rods and fuel assembly grid springs. Vibration and fretting forces vary during the fuel life due to clad diameter creep-down combined with grid spring relaxation.

d. Chemical Properties of the Cladding - This is discussed in Reference 4.2-2.

4.2.1.2 Fuel Material.

a. Thermal-Physical Properties

Fuel Pellet Temperatures - The center temperature of the hottest pellet is to be below the melting temperature of the UO_2 (melting point of 5080°F [Ref. 4.2-3] unirradiated and decreasing by 58°F per 10,000 MWd/MTU). While a limited amount of center melting can be tolerated, the design conservatively precludes center melting. A calculated fuel centerline temperature of 4700°F has been selected as an overpower limit to assure no fuel melting. This provides sufficient margin for uncertainties as described in Subsection 4.4.2.9.

The normal design density of the fuel is 95 percent of theoretical. Additional information on fuel properties is given in Reference 4.2-2.

b. Fuel Densification and Fission Product Swelling

The design bases and models used for fuel densification and swelling are provided in References 4.2-4 and 4.2-5.

c. Chemical Properties

These limits are applied to the design and evaluation of the top and bottom nozzles, guide thimbles, grids, and the thimble joints.

The design bases for evaluating the structural integrity of the fuel assemblies are:

a. Non-operational - 4 g axial and 6 g lateral loading with dimensional stability. 49

b. For the normal operating and upset conditions, the fuel assembly component structural design criteria are established for the two primary material categories, namely austenitic steels and Zircaloy. The stress categories and strength theory presented in the ASME B&PV Code, Section III, are used as a general guide. The maximum shear-theory (Tresca criterion) for combined stresses is used to determine the stress intensities for the austenitic steel components. The stress intensity is defined as the numerically largest difference between the various principal stresses in a three dimensional field. The allowable stress intensity value for austenitic steels, such as nickel-chromium-iron alloys, is given by the lowest of the following:

   1) One-third of the specified minimum tensile strength or 2/3 of the specified minimum yielded strength at room temperature

   2) One-third of the tensile strength or 90 percent of the yield strength at temperature but not to exceed 2/3 of the specified minimum yield strength at room temperature.

   The stress limits for the austenitic steel components are given below. All stress nomenclature is per the ASME B&PV Code, Section III.

Stress Intensity Limits

Categories	Limit
General Primary Membrane Stress Intensity	Sm
Local Primary Membrane Stress Intensity	1.5 Sm
Primary Membrane plus Bending Stress Intensity	1.5 Sm
Total Primary plus Secondary Stress Intensity	3.0 Sm

The Zircaloy structural components which consist of guide thimble and fuel tubes are in turn subdivided into two categories because of material differences and functional requirements. The fuel tube design criteria ~~is~~ are covered separately in Section 4.2.1.1. The maximum shear theory is used to evaluate the guide thimble des'gn. For conservative purposes, the Zircaloy unirradiated properties are used to define the stress limits.

1. Absorber Rods

The material properties and compatibilities are given in Refs. 4.2-2 and 4.2-7. The design bases include a stress intensity limit, Sm, of 2/3 of the 0.2 percent offset yield stress for the 304 stainless steel clad tubing during the 15 year minimum RCCA design life. The design basis of the absorber material is that it does not exceed its minimum melting point of 3913°F (Ref. 4.2-7). 30

2. Burnable Poison Rods

The burnable poison rod clad is designed as a Class 1 Component under Article NB-3000 of the ASME B&PV Code, Section III, 1973 for Conditions I and II. For abnormal loads during Conditions III and IV code stresses are not considered limiting. Failures of the burnable poison rods during these conditions must not interfere with reactor shutdown or cooling of the fuel rods.

The burnable poison absorber material is non-structural. The structural elements of the burnable poison rod are designed to maintain the absorber geometry even if the absorber material is fractured. The rods are designed so that the absorber material is below its softening temperature (1492°F* for reference 12.5 weight percent ~~without~~ boron rods). In addition, the structural elements are designed to prevent excessive slumping.

3. Neutron Source Rods

The neutron source rods are designed to withstand the following:

a. The external pressure equal to the Reactor Coolant System (RCS) operating pressure with appropriate allowance for overpressure transients and,

b. An internal pressure equal to the pressure generated by released gases over the source rod life.

4. Thimble Plug Assembly

The thimble plug assembly is needed to restrict bypass flow through those thimbles not occupied by absorber, source or burnable poison rods.

The thimble plug assemblies satisfy the following:

a. Accommodate the differential thermal expansion between the fuel assembly and the core internals,

b. Maintain positive contact with the fuel assembly and the core internals.

*Borosilicate glass is accepted for use in burnable poison rods if the softening temperature is 1510 ± 18°F. The softening temperature is defined in ASTM C 338.

and seal welded at the ends to encapsulate the fuel. A schematic of the fuel rod is shown in Figure 4.2-3. The fuel pellets are right circular cylinders consisting of slightly enriched uranium dioxide powder which has been compacted by cold pressing and then sintered to the required density. The ends of each pellet are dished slightly to allow greater axial expansion at the center of the pellets, and have a small chamfer at the outer cylinder surface.

To avoid overstressing of the clad or seal welds, void volume and clearances are provided within the rods to accommodate fission gases released from the fuel, differential thermal expansion between the clad and the fuel, and fuel density changes during irradiation. Shifting of the fuel within the clad during handling or shipping prior to core loading is prevented by a stainless steel helical spring which bears on top of the fuel. At assembly the pellets are stacked in the clad to the required fuel height, the spring is then inserted into the top end of the fuel tube and the end plugs pressed into the ends of the tube and welded. All fuel rods are internally pressurized with helium during the welding process in order to minimize compressive clad stresses and prevent clad flattening due to coolant operating pressures.

The fuel rods are presently being designed and pre-pressurized so that: 1) the internal gas pressure mechanical design limit given in Subsection 4.2.1.3 (B) is not exceeded and, 2) the cladding stress-strain limits (Subsection 4.2.1.1) are not exceeded for Condition I and II events, and 3) clad flattening will not occur during the fuel core life.

4.2.2.2 Fuel Assembly Structure. The fuel assembly structure consists of a bottom nozzle, top nozzle, guide thimbles and grids, as shown in Figure 4.2-2.

4.2.2.2.1 Bottom Nozzle: The bottom nozzle serves as a bottom structural element of the fuel assembly and directs the coolant flow distribution to the assembly. The square nozzle is fabricated from Type 304 stainless steel and consists of a perforated plate and four angle legs with bearing plates as shown in Figure 4.2-2. The legs form a plenum for the inlet coolant flow to the fuel assembly. The plate also prevents accidental downward ejection of the fuel rods from the fuel assembly. The bottom nozzle is fastened to the fuel assembly guide tubes by locked screws which penetrate through the nozzle and mate with a threaded plug in each guide tube. |30

Coolant flow through the fuel assembly is directed from the plenum in the bottom nozzle upward through the penetrations in the plate to the channels between the fuel rods. The penetrations in the plate are positioned between the rows of the fuel rods.

Axial loads (holddown) imposed on the fuel assembly and the weight of the fuel assembly are transmitted through the bottom nozzle to the lower core support structure. Indexing and positioning of the fuel assembly is controlled by alignment holes in two diagonally opposite bearing plates which mate with locating pins in the lower core support. Any lateral loads on the fuel assembly are transmitted to the lower core support through the locating pins.

The clad in the rod assemblies is slightly cold worked Type 304 stainless steel. All other structural materials are Types 304 or 308 stainless steel except for the springs which are Inconel-718. The borosilicate glass tube provides sufficient boron content to meet the criteria discussed in Section 4.3.1.

4.2.2.3.3 Neutron Source Assembly: The purpose of a neutron source assembly is to provide a base neutron level to ensure that the detectors are operational and responding to core multiplication neutrons. Since there is very little neutron activity during loading, refueling, shutdown, and approach to criticality, a neutron source is placed in the reactor to provide a positive neutron count of at least 2 counts per second on the source range detectors attributable to core neutrons. The detectors, called source range detectors, are used primarily when the core is subcritical and during special subcritical modes of operations.

The source assembly also permits detection of changes in the core multiplication factor during core loading refueling, and approach to criticality. This can be done since the multiplication factor is related to an inverse function of the detector count rate. Therefore a change in the multiplication factor can be detected during addition of fuel assemblies while loading the core, a change in control rod positions, and changes in boron concentration.

Both primary and secondary neutron source rods are used. The primary source rod, containing a radioactive material, spontaneously emits neutrons during initial core loading and reactor startup. After the primary source rod decays beyond the desired neutron flux level, neutrons are then supplied by the secondary source rod. The secondary source rod contains a stable material, which must be activated by neutron bombardment during reactor operation. The activation results in the subsequent release of neutrons. This becomes a source of neutrons during periods of low neutron flux, such as during refueling and subsequent startups.

The reactor core employs four source assemblies: two primary source assemblies and two secondary source assemblies. Each primary source assembly contains one primary source rod and a number of burnable poison rods. Each secondary source assembly contains a symmetrical grouping of four secondary source rods with ~~and may contain a number of burnable poison rods. Locations not~~ | 18
~~filled with a source or burnable poison rod contain a~~ thimble plugs in the remaining locations. The source assemblies are shown in Figures 4.2-13 and 4.2-14.

Neutron source assemblies are employed at opposite sides of the core. The assemblies are inserted into the rod cluster control guide thimbles in fuel assemblies at selected unrodded locations.

As shown in Figure~~s~~ 4.2-13~~, and 4.2-14~~, the primary source assembl~~ies~~y contains a hold-down assembly identical to that of the burnable poison assembly.

The secondary source assembly shown in Figure 4.2-14 contains a spider assembly. The spider assembly is in the form of a central hub with radial vanes containing cylindrical fingers from which the secondary source rods and thimble plugs are suspended.

The primary and secondary source rods utilize the same cladding material as the absorber rods. The secondary source rods contain antimony-beryllium pellets stacked to a height of approximately 88 in. The primary source rods contain capsules of californium (plutonium-beryllium possible alternate) source material and alumina spacer pellets to position the source material within the cladding. The rods in each assembly are permanently fastened ~~at~~ the top end to a holddown assembly.

The other structural members are constructed of Type 304 stainless steel except for the springs. The springs exposed to the reactor coolant are Inconel 718.

STET STET

4.2.2.3.4 Thimble Plug Assembly: In order to limit bypass flow through the rod cluster control guide thimbles in fuel assemblies which do not contain either control rods, source rods, or burnable poison rods, the fuel assemblies are fitted with thimble plug assemblies at those locations. assemblies

The thimble plug assemblies as shown in Figure 4.2-15 consist of a flat base plate with short rods suspended from the bottom surface and a spring pack assembly. The twenty-four short rods, called thimble plugs, project into the upper ends of the guide thimbles to reduce the bypass flow. Each thimble plug is permanently attached to the base plate by a nut which is lock-welded to the threaded end of the plug. Similar short rods are also used on the source assemblies and burnable poison assemblies to plug the ends of all vacant fuel assembly guide thimbles. At installation in core, the thimble plug assemblies interface with both the upper core plate and with the fuel assembly top nozzles by resting on the adaptor plate. The spring pack is compressed by the upper core plate when the upper internals assembly is lowered into place. upon

All components in the thimble plug assembly, except for the springs, are constructed from Type 304 stainless steel. The springs are Inconel 718.

4.2.3 Design Evaluation

Subsection
Section

The fuel assemblies and fuel rods are designed to satisfy the performance and safety criteria of 4.2, the mechanical design bases of 4.2.1, and other interfacing nuclear and thermal-hydraulic design bases specified in Sections 4.3 and 4.4. Effects of Accident Conditions II, III, IV or anticipated transients without trip (ATWT) on fuel integrity are presented in Chapter 15 or supporting topical reports. 30

The initial step in fuel rod design evaluation for a region of fuel is to determine the limiting rod(s). Limiting rods are defined as those rod(s) whose predicted performance provides the minimum margin to each of the design criteria. For a number of design criteria the limiting rod is the lead burnup rod of a fuel region. In other instances it may be the maximum power or the minimum burnup rod. For the most part, no single rod will be limiting with respect to all design criteria.

ATTACHMENT 1
ST-HL-AE-1432
PAGE 10 OF 54

3140-7

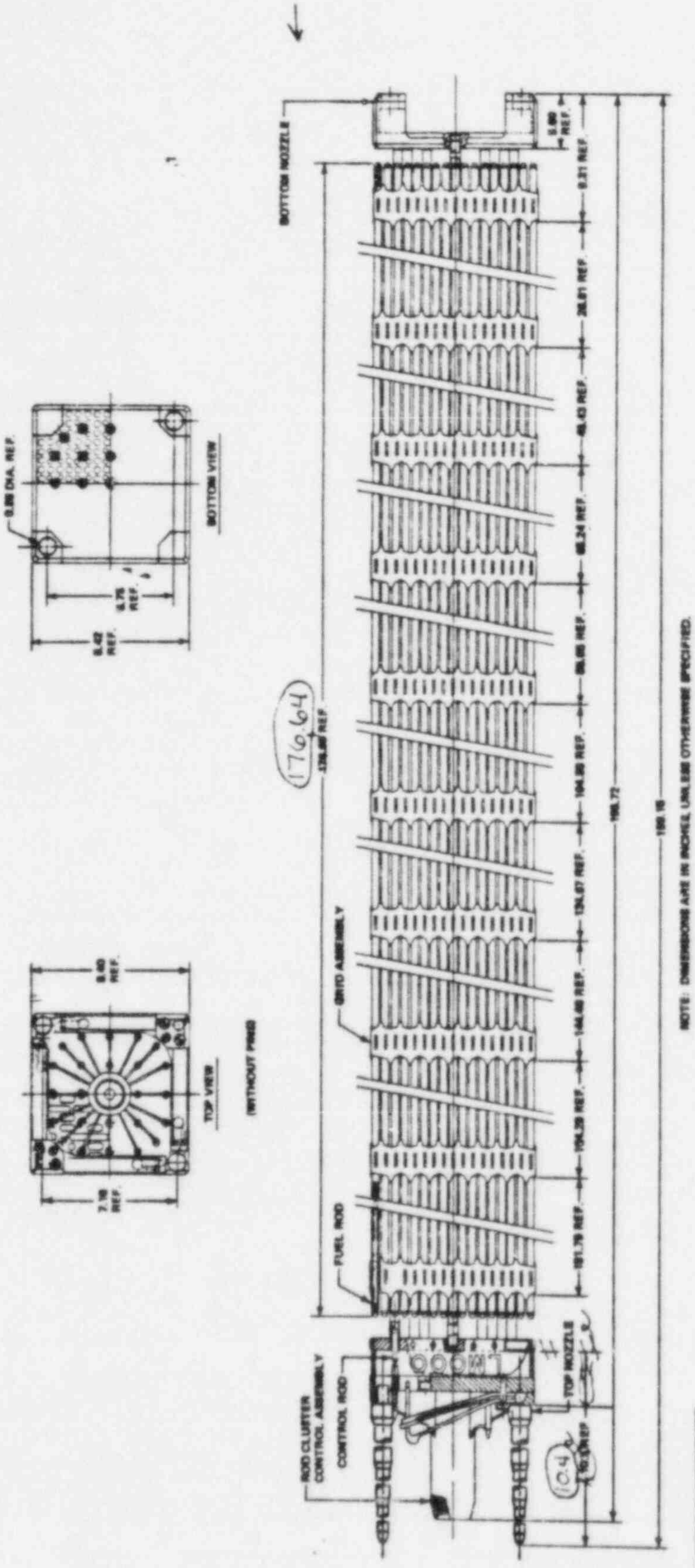

SOUTH TEXAS PROJECT UNITS 1 & 2

FUEL ASSEMBLY OUTLINE
17 X 17 XL (CONCEPTUAL)

FIGURE 4.2-2

Amendment 30

3140-5

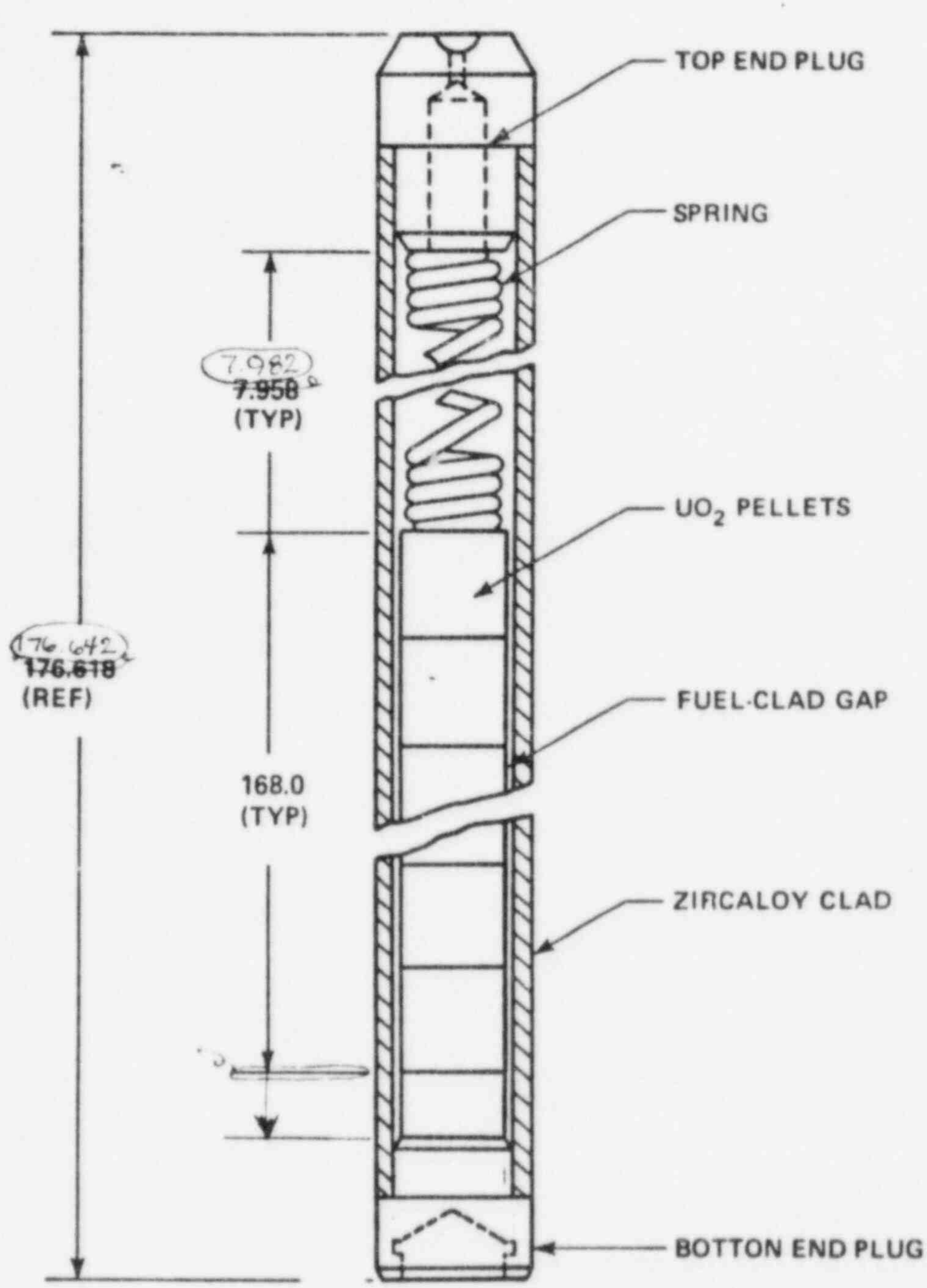

SPECIFIC DIMENSIONS DEPEND ON DESIGN VARIABLES SUCH AS PRE-PRESSURIZATION, POWER HISTORY, AND DISCHARGE BURNUP

SOUTH TEXAS PROJECT
UNITS 1 & 2

FUEL ROD SCHEMATIC

FIGURE 4.2-3

Amendment 30

ATTACHMENT 1
ST-HL-AE-1432
PAGE 12 OF 54

3140-1

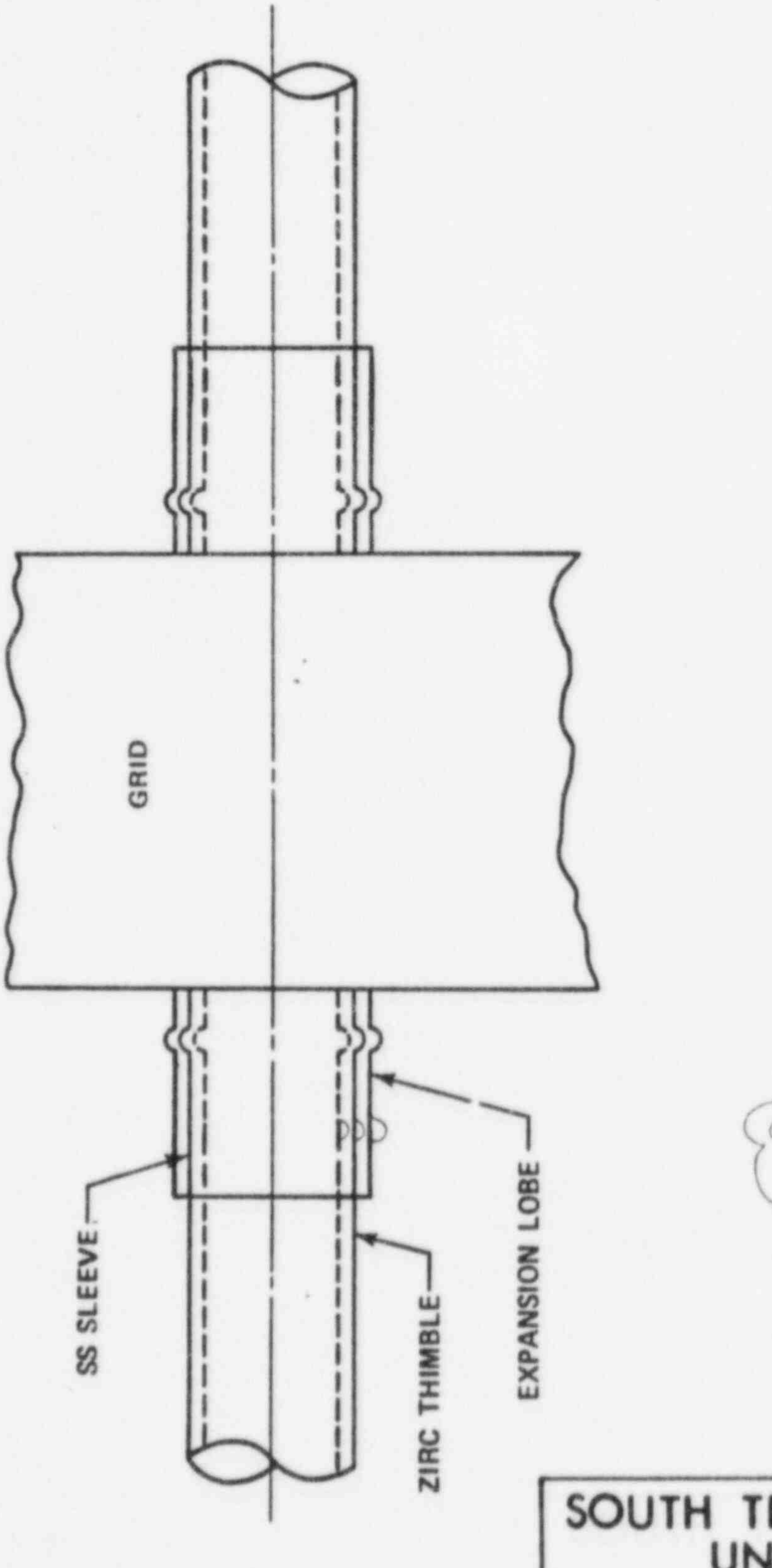

SOUTH TEXAS PROJECT
UNITS 1 & 2

ELEVATION VIEW

FIGURE 4.2-5

Amendment 30

3140-4

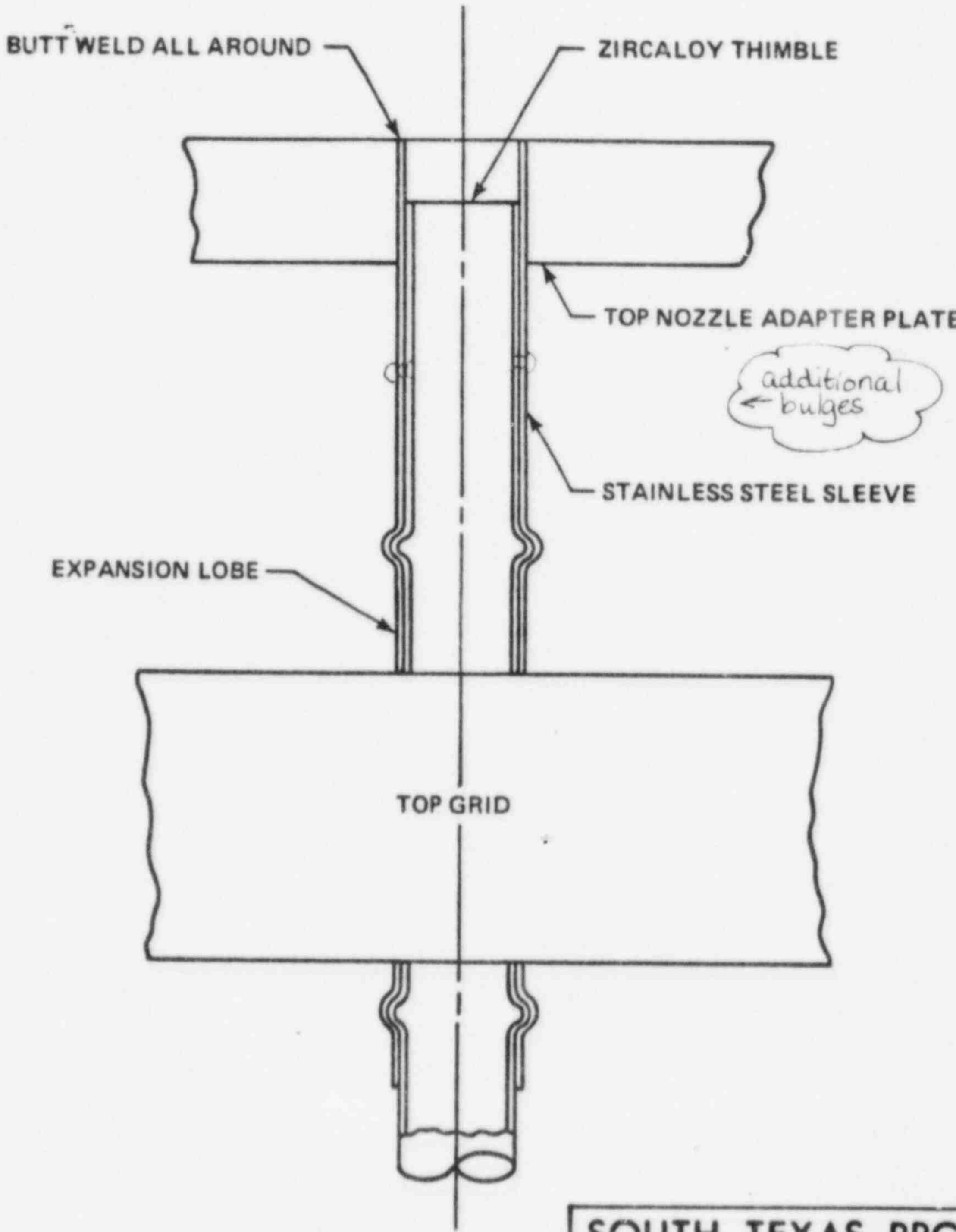

SOUTH TEXAS PROJECT
UNITS 1 & 2

TOP GRID NOZZLE ATTACHMENT

FIGURE 4.2-6

Amendment 30

15,591-6

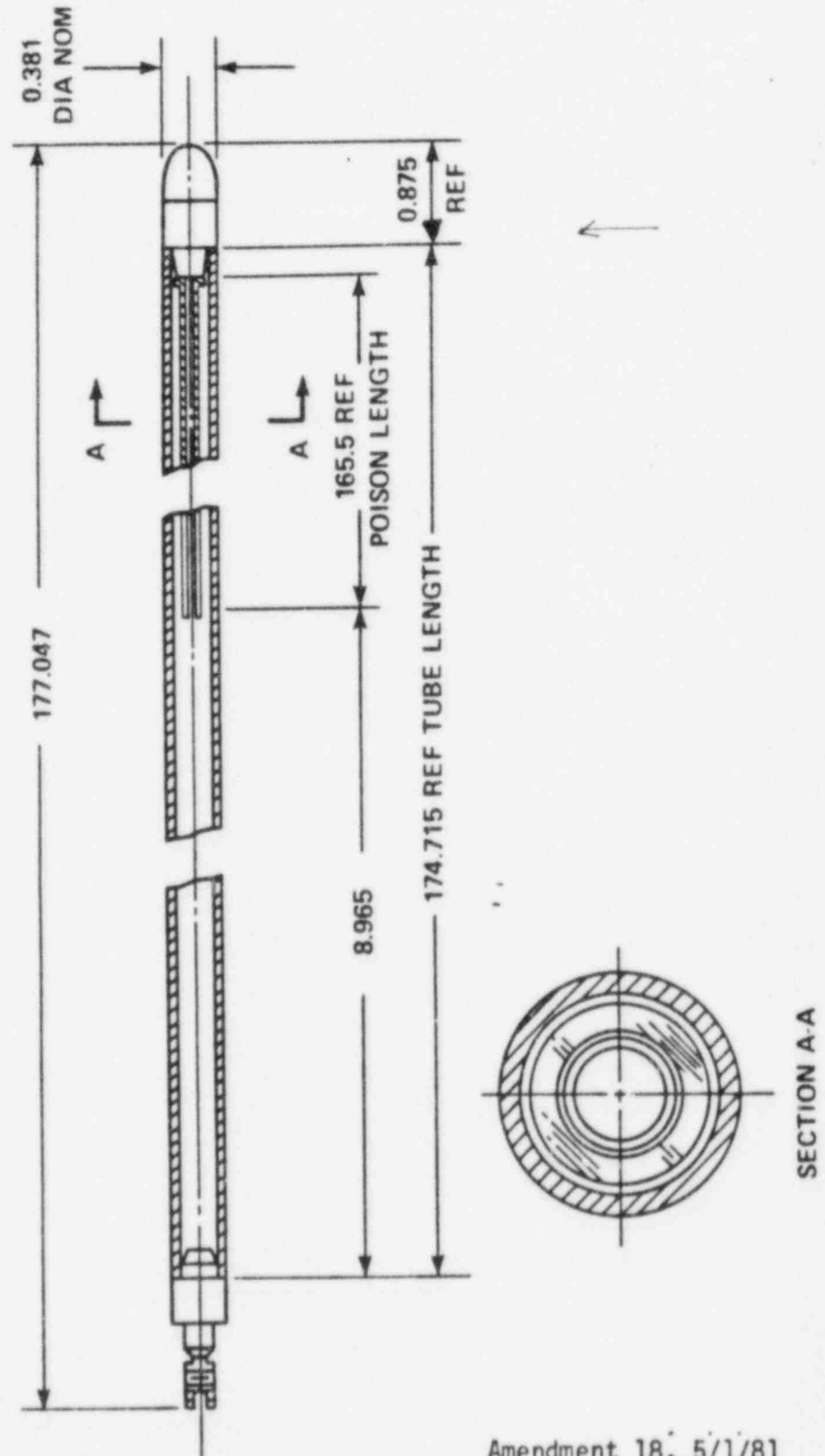

Amendment 18, 5/1/81

SOUTH TEXAS PROJECT
UNITS 1 & 2

Figure 4.2-12.

Burnable Poison Rod-Cross Section

ATTACHMENT 1
ST-HL-AE-1432
PAGE 15 OF 54

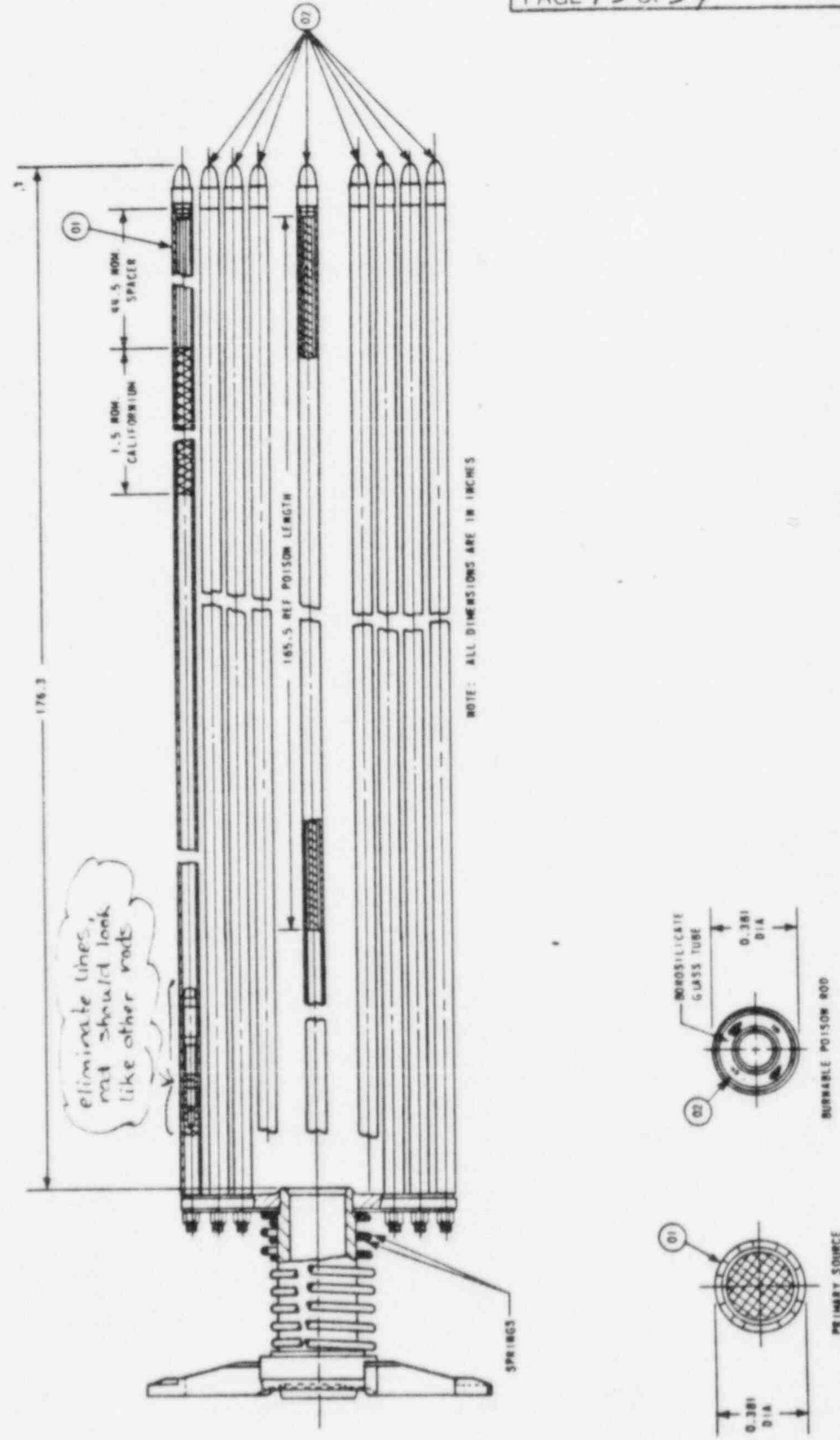

Amendment 18, 5/1/81

SOUTH TEXAS PROJECT
UNITS 1 & 2

Figure 4.2-13.
Primary Source Assembly

ATTACHMENT 1
ST-HL-AE-1432
PAGE 16 OF 54

Replace with new Figure

3140-13

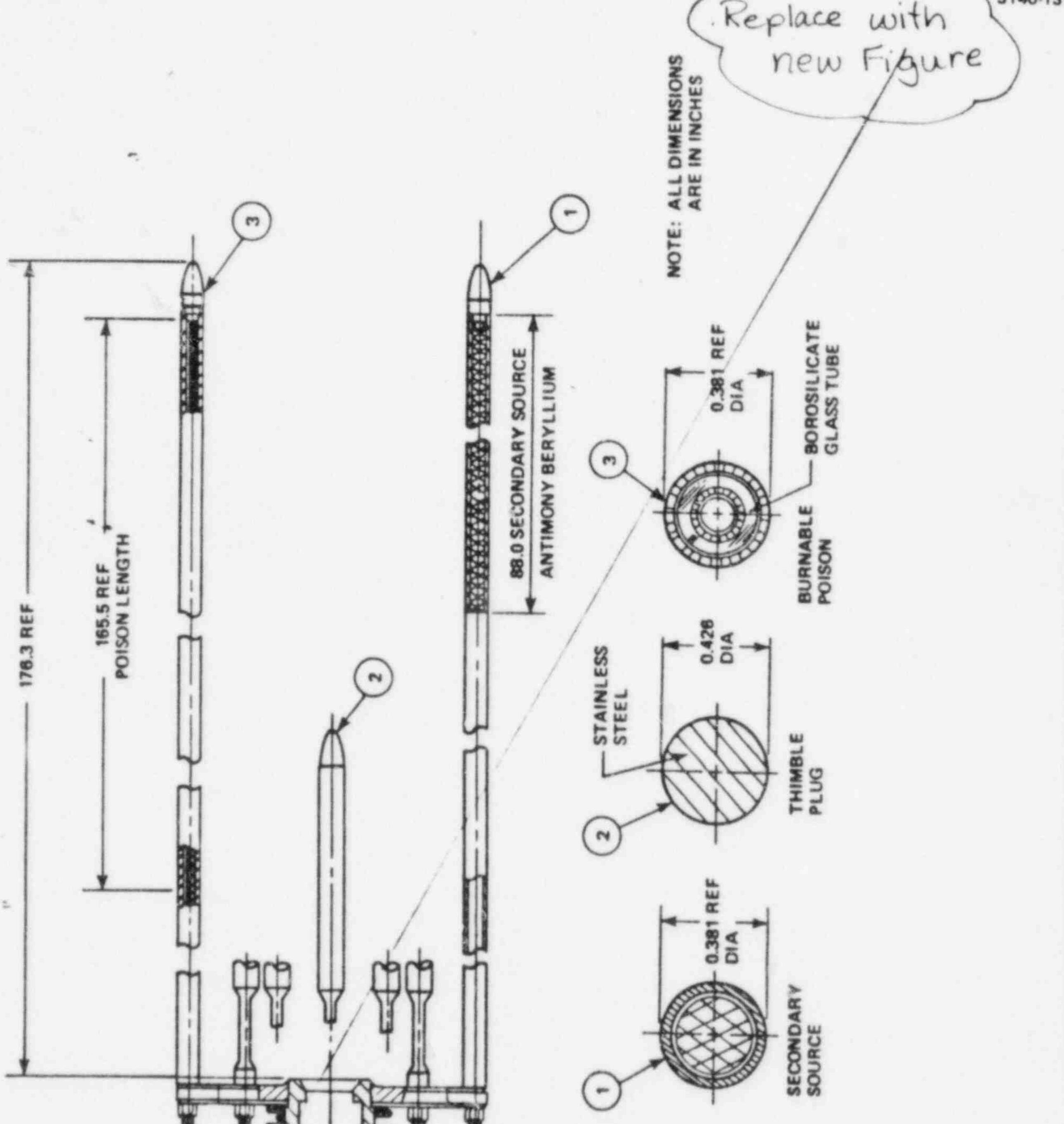

SOUTH TEXAS PROJECT
UNITS 1 & 2

SECONDARY SOURCE ASSEMBLE

FIGURE 4.2-14

Amendment 30

Revised Figure

3140-13

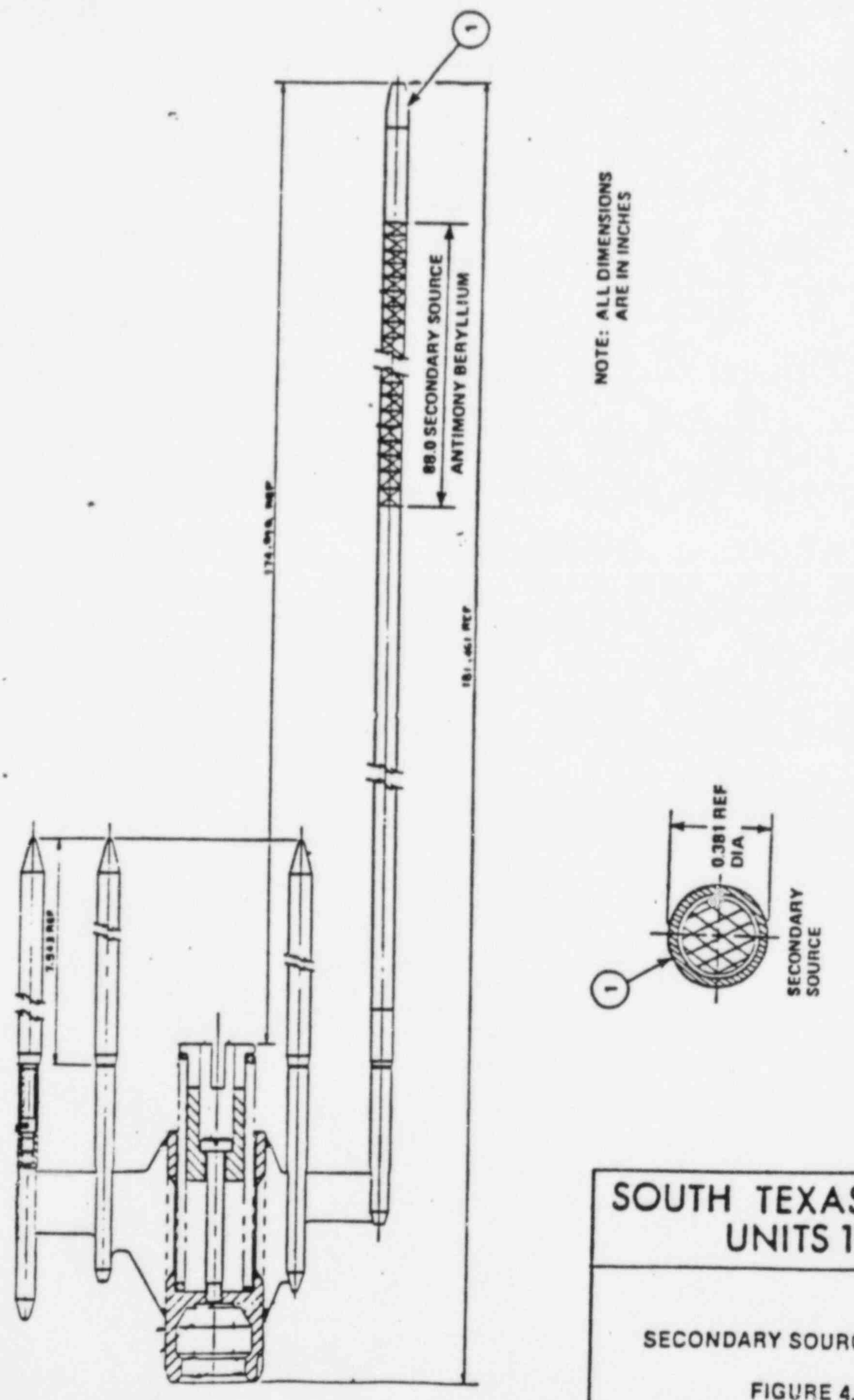

SOUTH TEXAS PROJECT
UNITS 1 & 2

SECONDARY SOURCE ASSEMBLY

FIGURE 4.2-14

Amendment 30

3140-10

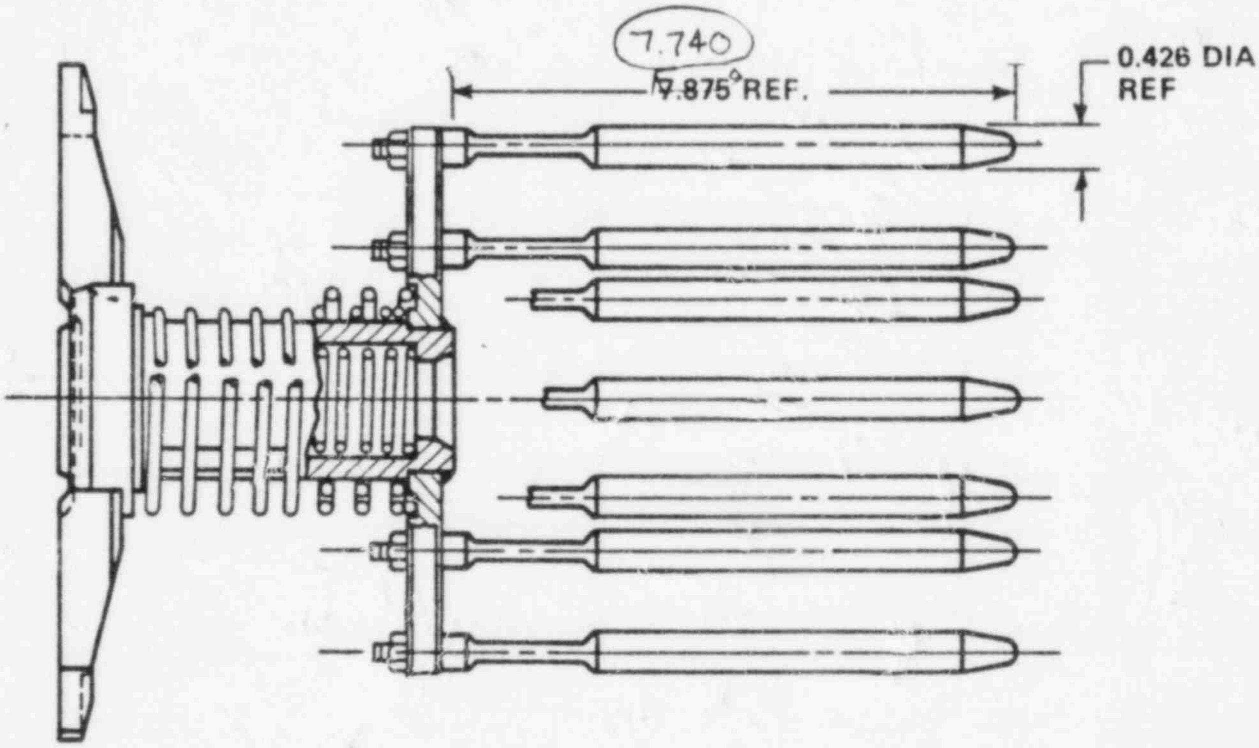

SOUTH TEXAS PROJECT
UNITS 1 & 2

THIMBLE PLUG
ASSEMBLY (CONCEPTUAL)

FIGURE 4.2-15

Amendment 30

ATTACHMENT 1
ST-HL-AE-1432
PAGE 19 OF 54

reactivity compensation. The core is also designed to have an overall negative moderator temperature coefficient of reactivity so that average coolant temperature or void content provides another, slower compensatory effect. Nominal power operation is permitted only in a range of overall negative moderator temperature coefficient. The negative moderator temperature coefficient can be achieved through use of fixed burnable poison and/or control rods by limiting the reactivity held down by soluble boron.

Burnable poison content (quantity and distribution) is not stated as a design basis other than as it relates to accomplishment of a non-positive moderator temperature coefficient at power operating conditions discussed above.

4.3.1.3 Control of Power Distribution.

Basis

The nuclear design basis is that, with at least a 95 percent confidence level:

1. The fuel will not be operated at greater than 13.3 KW/ft under normal operating conditions including an allowance of 2 percent for calorimetric error and not including power spike factor due to densification.

2. Under abnormal conditions including the maximum overpower condition, the fuel peak power will not cause melting as defined in Subsection 4.4.1.2.

3. The fuel will not operate with a power distribution that violates the departure from nucleate boiling (DNB) design basis (i.e., the DNBR shall not be less than ~~1.28~~ 1.30, as discussed in Section 4.4.1) under Condition I and II events including the maximum overpower condition.

4. Fuel management will be such as to produce rod powers and burnups consistent with the assumptions in the fuel rod mechanical integrity analysis of Section 4.2.

The above basis meets GDC10.

Discussion

Calculation of extreme power shapes which affect fuel design limits is performed with proven methods and verified frequently with measurements from operating reactors. The conditions under which limiting power shapes are assumed to occur are chosen conservatively with regard to any permissible operating state.

Even though there is good agreement between measured peak power calculations and measurements, a nuclear uncertainty margin (Subsection 4.3.2.2-7) is applied to calculated peak local power. Such a margin is provided both for the analysis for normal operating states and for anticipated transients.

ATTACHMENT 1
ST-HL-AE-1432
PAGE 20 OF 54

Limits for alarms, reactor trip, etc. will be given in the Technical Specifications. Descriptions of the systems provided are given in Section 7.7. | 27

4.3.2.3 Reactivity Coefficients. The kinetic characteristics of the reactor core determine the response of the core to changing plant conditions or to operator adjustments made during normal operation, as well as the core response during abnormal or accidental transients. These kinetic characteristics are quantified in reactivity coefficients. The reactivity coefficients reflect the changes in the neutron multiplication due to varying plant conditions such as power, moderator or fuel temperatures, or less significantly due to a change in pressure or void conditions. Since reactivity coefficients change during the life of the core, ranges of coefficients are employed in transient analysis to determine the response of the plant throughout life. The results of such simulations and the reactivity coefficients used are presented in Chapter 15. The reactivity coefficients are calculated on a corewise basis by radial and axial diffusion theory methods. The effect of radial and axial power distribution on core average reactivity coefficients is implicit in those calculations and is not significant under normal operating conditions. For example, a skewed xenon distribution which results in changing axial offset by 5 percent changes the moderator and Doppler temperature coefficients by less than 0.01 pcm/°F and 0.03 pcm/°F respectively. An artificialy skewed xenon distribution which results in changing the radial $F^N_{\Delta H}$ by 3 percent changes the moderator and Doppler temperature coefficients by less than 0.03 pcm/°F and 0.001 pcm/°F respectively. The spatial effects are accentuated in some transient conditions; for example, in postulated rupture of the main steamline break and rupture of RCCA mechanism housing described in Sections 15.1.5 and 15.4.8, and are included in these analyses.

The analytical methods and calculational models used in calculating the reactivity coefficients are given in Section 4.3.3. These models have been confirmed through extensive testing of more than thirty cores similar to the plant described herein; results of these tests are discussed in Section 4.3.3.

Quantitative information for calculated reactivity coefficients, including fuel Doppler coefficient, moderator coefficients (density, temperature, pressure, void) and power coefficient is given in the following sections.

The reactivity requirements at EOL of a typical cycle for a 168 in and a 144 in 17 x 17 four loop core are listed on a comparable basis in Table 4.3-4. The Doppler defect is slightly less for the 168 in core due to the lower average linear power density (5.20 vs. 5.44 Kw/ft). The moderator defect is higher due to the slightly more negative moderator temperature coefficient at the higher temperature of the 168 in core. The redistribution requirement is greater for the longer core (1.20 percent $\Delta\rho$ vs. 0.85 percent $\Delta\rho$). More excess margin is available to the 168 in core than the 12 ft core due to the use of 57 rather than 53 control rods in this example. Both cores operate in the same range of expected reactivity parameters as shown in Table 4.3-5.

¶ moved to section 4.3.2.4.8

4.3.2.3.1 Fuel Temperature (Doppler) Coefficient: The fuel temperature (Doppler) coefficient is defined as the change in reactivity per degree change in effective fuel temperature and is primarily a measure of the Doppler broadening of uranium-238 and plutonium-240 resonance absorption peaks. Doppler broadening of other isotopes such as uranium-236, neptunium-237 etc. are also considered but their contributions to the Doppler effect is small. An increase in fuel temperature increases the effective resonance absorption cross sections of the fuel and produces a corresponding reduction in reactivity.

The fuel temperature coefficient is calculated by performing two-group X-Y calculations using an updated version of the TURTLE[4.3-12] Code. Moderator temperature is held constant and the power level is varied. Spatial variation of fuel temperature is taken into account by calculating the effective fuel temperature as a function of power density as discussed in Subsection 4.3.3.1.

The Doppler temperature coefficient is shown on Figure 4.3-27 as a function of the effective fuel temperature (at BOL and EOL conditions). The effective fuel temperature is lower than the volume averaged fuel temperature since the neutron flux distribution is non-uniform through the pellet and gives preferential weight to the surface temperature. The Doppler-only contribution to the power coefficient, defined later, is shown on Figure 4.3-28 as a function of relative core power. The integral of the differential curve on Figure 4.3-28 is the Doppler contribution to the power defect and is shown on Figure 4.3-29 as a function of relative power. The Doppler coefficient becomes more negative as a function of life as the plutonium-240 content increases, thus increasing the plutonium resonance absorption, but overall becomes less negative since the fuel temperature changes with burnup as described in Subsection 4.3.3.1. The upper and lower limits of Doppler coefficient used in accident analyses are given in Chapter 15.

4.3.2.3.2 Moderator Coefficients: The moderator coefficient is a measure of the change in reactivity due to a change in specific coolant parameters such as density, temperature, pressure or void. The coefficients so obtained are moderator density, temperature, pressure and void coefficients.

Moderator Density and Temperature Coefficients

The moderator temperature (density) coefficient is defined as the change in reactivity per degree change in the moderator temperature. Generally, the effect of the changes in moderator density as well as the temperature are considered together. A decrease in moderator density means less moderation which results in a negative moderator coefficient. An increase in coolant temperature, keeping the density constant, leads to a hardened neutron spectrum and results in an increase in resonance absorption in uranium-238, plutonium-240 and other isotopes. The hardened spectrum also causes a decrease in the fission to capture ratio in uranium-235 and plutonium-239. Both of these effects make the moderator coefficient more negative. Since water density changes more rapidly with temperature as temperature increases, the moderator temperature coefficient become more negative with increasing temperature.

The soluble boron used in the reactor as a means of reactivity control also has an effect on moderator temperature ~~density~~ coefficient since the soluble boron poison density as well as the water density is decreased when the coolant temperature rises. ~~A decrease~~ An increase in the soluble poison concentration introduces a positive component in the moderator temperature coefficient.

Thus, if the concentration of soluble poison is large enough, the net value of the coefficient may be positive. With the burnable poison rods present, however, the initial hot boron concentration is sufficiently low that the moderator temperature coefficient is negative at operating temperatures. The effect of control rods is to make the moderator temperature coefficient more negative by reducing the required soluble boron concentration and by increasing the "leakage" of the core.

With burnup, the moderator temperature coefficient becomes more negative primarily as a result of boric acid dilution but also to a significant extent from the effects of the buildup of plutonium and fission products.

The moderator temperature coefficient is calculated for the various plant conditions discussed above by performing two-group X-Y calculations, varying the moderator temperature by about ± 5°F about each of the mean temperatures. The moderator temperature coefficient is shown as a function of core temperature and boron concentration for the unrodded and rodded core on Figures 4.3-30 through 4.3-32. The temperature range covered is from cold (68°F) to about 600°F. The contribution due to Doppler coefficient (because of change in moderator temperature) has been subtracted from these results. Figure 4.3-33 shows the hot, full power moderator temperature coefficient plotted as a function of first cycle lifetime for the just critical boron concentration condition based on Figure 4.3-3.

The moderator temperature (density) coefficients presented here are calculated on a corewide basis, since they are used to describe the core behavior in normal and accident situations when the moderator temperature changes can be considered to affect the entire core. Moderator temperature coefficient and moderator density coefficient are used interchangeably according to which is more appropriate as input for the codes used.

Moderator Pressure Coefficient

The moderator pressure coefficient relates the change in moderator density, resulting from a reactor coolant pressure change, to the corresponding effect on neutron production. This coefficient is of much less significance in comparison with the moderator temperature coefficient. A change of 50 psi in pressure has approximately the same effect on reactivity as a half-degree change in moderator temperature. This coefficient can be determined from the moderator temperature coefficient by relating change in pressure to the corresponding change in density. The moderator pressure coefficient is negative over a portion of the moderator temperature range at BOL (-0.004 pcm/psi, BOL) but is always positive at operating conditions and becomes more positive during life (+0.3 pcm/psi, EOL). Due principally to the change in boron concentration of the moderator with cycle burnup.

Moderator Void Coefficient

The moderator void coefficient relates the change in neutron multiplication to the presence of voids in the moderator. In a PWR this coefficient is not very significant because of the low void content in the coolant. The core void content is less than one-half of one percent and is due to local or statistical boiling. The void coefficient varies from 50 pcm/percent void at BOL and at low temperatures to -250 pcm/percent void at EOL and at operating temperatures. The negative void coefficient at operating temperature becomes more negative with fuel burnup.

4.3.2.3.3 Power Coefficient: The combined effect of moderator temperature and fuel temperature change as the core power level changes is called the total power coefficient and is expressed in terms of reactivity change per percent power change. The power coefficient at BOL and EOL conditions is given on Figure 4.3-34.

It becomes more negative with burnup reflecting the combined effect of moderator and fuel temperature coefficients with burnup. The power defect (integral reactivity effect) at BOL and EOL is given on Figure 4.3-35.

4.3.2.3.4 Comparison of Calculated and Experimental Reactivity Coefficients: Section 4.3.3 describes the comparison of calculated and experimental reactivity coefficients in detail. Based on the data presented there, the accuracy of the current analytical model is:

$\pm$0.2 percent $\Delta\rho$ for Doppler and power defect
$\pm$2 pcm/°F for the moderator coefficient.

Experimental evaluation of the calculated coefficients will be completed during the physics startup tests described in Chapter 14.

4.3.2.3.5 Reactivity Coefficients Used in Transient Analysis: Table 4.3-2 gives the limiting values as well as the best estimate values for the reactivity coefficients. The limiting values are used as design limits in the transient analysis. The exact values of the coefficient used in the analysis depend on whether the transient of interest is examined at ~~the~~ BOL or EOL, whether the most negative or the most positive (least negative) coefficients are appropriate, and whether spatial nonuniformity must be considered in the analysis. Conservative values of coefficients, considering various aspects of analysis are used in the transient analysis. This is described in Chapter 15.

effective pellet temperature. This effect is most noticeable over the range of zero power to full power due to the large pellet temperature increase with power generation.

4.3.2.4.2 Variable Average Moderator Temperature: When the core is shutdown to the hot zero power (HZP) condition, the average moderator temperature changes from the equilibrium full load value determined by the steam generator and turbine characteristics (steam pressure, heat transfer, tube fouling, etc.) to the equilibrium no load value, which is based on the steam generator shell side design pressure. The design change in temperature is conservatively increased by 4°F to account for the control dead band and measurement errors.

Since the moderator temperature coefficient is negative, there is a reactivity addition with power reduction. The moderator temperature coefficient becomes more negative as the fuel depletes because the boron concentration is reduced. This effect is the major contributor to the increased requirement at EOL.

4.3.2.4.3 Redistribution: During full power operation the coolant density decreases with core height, and this, together with partial insertion of control rods, results in less fuel depletion near the top of the core. Under steady state conditions, the relative power distribution will be slightly asymmetric towards the bottom of the core. On the other hand, at hot zero power conditions, the coolant density is uniform up the core, and there is no flattening due to Doppler. The result will be a flux distribution which at zero power can be skewed toward the top of the core. The reactivity insertion due to the skewed distribution is calculated with an allowance for effects of xenon distribution. 30

4.3.2.4.4 Void Content: A small void content in the core is due to nucleate boiling at full power. The void collapse coincident with power reduction makes a small reactivity contribution.

4.3.2.4.5 Rod Insertion Allowance: At full power, the control bank is operated within a prescribed band of travel to compensate for small periodic changes in boron concentration, changes in temperature and very small changes in the xenon concentration not compensated for by a change in boron concentration. When the control bank reaches either limit of this band, a change in boron concentration is required to compensate for additional reactivity changes. Since the insertion limit is set by a rod travel limit, a conservatively high calculation of the inserted worth is made which exceeds the normally inserted reactivity.

4.3.2.4.6 Burnup: Excess reactivity of 10 percent $\Delta\rho$ (hot) is installed at the beginning of each cycle to provide sufficient reactivity to compensate for fuel depletion and fission products throughout the cycle. This reactivity is controlled by the addition of soluble boron to the coolant and by burnable poison(s). The soluble boron concentration for several core configurations, the unit boron worth, and burnable poison worth are given in Tables 4.3-1 and 4.3-2. Since the excess reactivity for burnup is controlled by soluble boron and/or burnable poison, it is not included in control rod requirements.

and pH effects

4.3.2.4.7 Xenon and Samarium Poisoning: Changes in xenon and samarium concentrations in the core occur at a sufficiently slow rate, even following rapid power level changes, that the resulting reactivity change is controlled by changing the soluble boron concentration.

9
4.3.2.4.8 pH effects: Changes in reactivity due to a change in coolant pH, if any, are sufficiently small in magnitude and occur slowly enough to be controlled by the boron system. Further details are provided in Reference 4.3-13.

INSERT 4.3.2.4.8

4.3.2.4.9 Experimental Confirmation: Following a normal shutdown, the total core reactivity change during cooldown with a stuck rod has been measured on a 121 assembly, 10 ft high core and 121 assembly, 12 ft high core. In each case, the core was allowed to cooldown until it reached criticality simulating the steamline break accident. For the 10 ft core, the total reactivity change associated with the cooldown is overpredicted by about 0.3 percent $\Delta\rho$ with respect to the measured result. This represents an error of about 5 percent in the total reactivity change and is about half the uncertainty allowance for this quantity. For the 12 ft core, the difference between the measured and predicted reactivity change was an even smaller 0.2 percent $\Delta\rho$. These measurements and others demonstrate the ~~ability~~ capability of the methods described in Section 4.3.3

4.3.2.4.10 Control: Core reactivity is controlled by means of a chemical poison dissolved in the coolant, RCCA's, and burnable poison rods as described below.

4.3.2.4.11 Chemical Poison: Boron in solution as boric acid is used to control relatively slow reactivity changes associated with:

1. The moderator temperature defect in going from cold shutdown at ambient temperature to the hot operating temperature at zero power,

2. The transient xenon and samarium poisoning, such as that following power changes or changes in rod cluster control position,

3. The excess reactivity required to compensate for the effects of fissile inventory depletion and buildup of long-life fission products.

4. The burnable poison depletion.

The boron concentrations for various core conditions are presented in Table 4.3-2.

INSERT for page 4.3-26

4.3.2.4.8 Combined Control Requirements:

inch — The reactivity requirements at EOL of a typical cycle for a 168 ~~in~~ inch and a 144 ~~in~~ 17 x 17 four loop core are listed on a comparable basis in Table 4.3-4. The Doppler defect is slightly less for the 168 ~~in~~ inch core due to the lower average linear power density (5.20 vs. 5.44 Kw/ft). The moderator defect is higher due to the slightly more negative moderator temperature coefficient at the higher temperature of the 168 ~~in~~ inch core. The redistribution requirement is greater for the longer core (1.20 percent $\Delta\rho$ vs. 0.85 percent $\Delta\rho$). More excess margin is available to the 168 ~~in~~ core inch than the 12 ft core due to the use of 57 rather than 53 control rods in this example. Both cores operate in the same range of expected reactivity parameters as shown in Table 4.3-5.

4.3.2.4.12 <u>Rod Cluster Control Assemblies</u>: Only Full-length assemblies are employed ~~exclusively~~ in this reactor. The number of assemblies is shown in Table 4.3-1. The RCCA's are used for shutdown and control purposes to offset fast reactivity changes associated with: 27

1. The required shutdown margin in the hot zero power, stuck rod condition,

2. The reactivity compensation as a result of an increase in power above hot zero power (power defect including Doppler, and moderator reactivity changes),

3. Unprogrammed fluctuations in boron concentration, coolant temperature, or xenon concentration (with rods not exceeding the allowable rod insertion limits),

4. Reactivity ramp rates resulting from load changes.

The allowed control bank reactivity insertion is limited at full power to maintain shutdown capability. As the power level is reduced, control rod reactivity requirements are also reduced and more rod insertion is allowed. The control bank position is monitored and the operator is notified by an alarm if the limit is approached. The determination of the insertion limit uses conservative xenon distributions and axial power shapes. In addition, the RCCA withdrawal pattern determined from these analyses is used in determining power distribution factors and in determining the maximum worth of an inserted RCCA ejection accident. Further discussion will be provided in the Technical Specifications on rod insertion limits. 27

Power distribution, rod ejection and rod misalignment analyses are based on the arrangement of the shutdown and control groups of the RCCA's shown on Figure 4.3-36. All shutdown RCCA's are withdrawn before withdrawal of the control banks is initiated. In going from zero to 100 percent power, control banks A, B, C and D are withdrawn sequentially. The limits of rod positions and further discussion on the basis for rod insertion limits will be provided in the Technical Specifications. 27

4.3.2.4.13 <u>Reactor Coolant Temperature</u>: Reactor coolant (or moderator) temperature control has added flexibility in reactivity control of the Westinghouse PWR. This feature takes advantage of the negative moderator temperature coefficient inherent in a PWR to:

1. Maximize return to power capabilities

2. Provide ± 5 percent power load regulation capabilities without requiring control rod compensation

3. Extend the time in cycle life to which daily load follow operations can be accomplished

ATTACHMENT 1
ST-HL-AE-1432
PAGE 28 OF 54

Reactor coolant temperature control supplements the dilution capability of the plant by lowering the reactor coolant temperature to supply positive reactivity through the negative moderator temperature coefficient of the reactor. After the transient is over, the system automatically recovers the reactor coolant temperature to the programmed value.

Moderator temperature control of reactivity, like soluble boron control, has the advantage of not significantly affecting the core power distribution. However, unlike boron control, temperature control can be rapid enough to achieve reactor power change rates of 5 percent/minute.

4.3.2.4.14 Burnable Poison Rods: The burnable poison rods provide partial control of the excess reactivity available during the first fuel cycle. In doing so, these rods prevent the moderator temperature coefficient from being positive at normal operating conditions. They perform this function by reducing the requirement for soluble poison in the moderator at the beginning of the first fuel cycle as described previously. For purposes of illustration a typical burnable poison rod pattern in the core together with the number of rods per assembly is shown on Figure 4.3-5, while the arrangements within an assembly are displayed on Figure 4.3-4. The reactivity worth of these rods is shown in Table 4.3-1. The boron in the rods is depleted with burnup but at a sufficiently slow rate so that the resulting critical concentration of soluble boron is such that the moderator temperature coefficient remains negative at all times for power operating conditions.

4.3.2.4.15 Peak Xenon Startup: Compensation for the peak xenon buildup is accomplished using the boron control system. Startup from the peak xenon condition is accomplished with a combination of rod motion and boron dilution. The boron dilution may be made at any time, including during the shutdown period, provided the shutdown margin is maintained.

4.3.2.4.16 Load Follow Control and Xenon Control: During load follow maneuvers, power changes are accomplished using control rod motion and dilution or boration by the boron system as required. Control rod motion is limited by the control rod insertion limits in the Technical Specifications 30
and discussed in Subsections 4.3.2.4.12 and 4.3.2.4.13. The power distribution is maintained within acceptable limits through the location of the rod 30
bank. Reactivity changes due to the changing xenon concentration can be controlled by rod motion and/or changes in the soluble boron concentration.

Late in cycle life, extended load follow capability is obtained by augmenting the limited boron dilution capability at low soluble boron concentrations by temporary moderator temperature reductions.

Rapid power increases (5 percent/minute) from part power during load follow operation are accomplished with a combination of rod motion, moderator temperature reduction, and boron dilution. Compensation for the rapid power increase is accomplished initially by a combination of rod withdrawal and moderator temperature reduction. As the slower boron dilution takes affect after the initial rapid power increase, the moderator temperature returns to the programmed value.

4.3.2.4.17 Burnup: Control of the excess reactivity for burnup is accomplished using soluble boron and/or burnable poison. The boron concentration must be limited during operating conditions to ensure the moderator temperature coefficient is negative. Sufficient burnable poison is installed at the beginning of a cycle to give the desired cycle lifetime without exceeding the boron concentration limit. The practical minimum boron concentration is 10 ppm.

4.3.2.5 Control Rod Patterns and Reactivity Worth. The RCCAs are designated by function as the control groups and the shutdown groups. The terms "group" and "bank" are used synonymously throughout this report to describe a particular grouping of control assemblies. The rod cluster assembly pattern is displayed on Figure 4.3-36. The control banks are labeled A, B, C, and D and the shutdown banks are labeled SA, SB, etc., as applicable. Each bank, although operated and controlled as a unit is comprised of two subgroups. The axial position of the RCCAs may be controlled manually or automatically. The RCCAs are all dropped into the core following actuation of reactor trip signals. |27

Two criteria have been employed for selection of the control groups. First, the total reactivity worth must be adequate to meet the requirements specified in Table 4.3-3. Second, in view of the fact that these rods may be partially inserted at power operation, the total power peaking factor should be low enough to ensure that the power capability requirements are met. Analyses indicate that the first requirement can be met either by a single group or by two or more banks whose total worth equals at least the required amount. The axial power shape would be more peaked following movement of a single group of rods worth three to four percent $\Delta\rho$ than following movement of more banks each worth less; therefore, four banks (described as A, B, C, and D on Figure 4.3-36) each worth approximately one percent $\Delta\rho$ have been selected. Typical control bank worths are shown in Table 4.3-2. |18

The position of control banks for criticality under any reactor condition is determined by the concentration of boron in the coolant. On an approach to criticality, boron is adjusted to ensure that criticality will be achieved with control rods above the insertion limit set by shutdown and other considerations which will be given in the Technical Specifications. Early in some cycles there may also be a withdrawal limit at low power to maintain a negative moderator temperature coefficient. As xenon and other fission products accumulate, this restriction is relaxed. However for the reference final core design described in this chapter, no such withdrawal limit is required. |27

Ejected rod worths are given in Section 15.4.8 for several different conditions.

Allowable deviations due to misaligned control rods will be discussed in the Technical Specifications. |27

Confirmatory critical experiments on burnable poisons are described in Reference 4.3-30. ②

4.3.3.3 Spatial Few-Group Diffusion Calculations. Spatial few-group calculations consist primarily of two-group diffusion X-Y calculations using an updated version of the TURTLE Code, two-group x-y nodal calculation using an updated version of the FLARE(32) code, and two-group axial calculations using an updated version of the PANDA Code.
the PALADON [4.3-33] code,

Discrete X-Y calculations (1 mesh per cell) are carried out to determine critical boron concentrations and power distributions in the X-Y plane. An axial average in the X-Y plane is obtained by synthesis from unrodded and rodded planes. Axial effects in unrodded depletion calculations are accounted for by the axial buckling, which varies with burnup and is determined by radial depletion calculations which are matched in reactivity to the analogous R-Z depletion calculation. The moderator coefficient is evaluated by varying the inlet temperature in the same X-Y calculations used for power distribution and reactivity predictions.

Validation of TURTLE reactivity calculations is associated with the validation of the group constants themselves, as discussed in Subsection 4.3.3.2. Validation of the Doppler calculations is associated with the fuel temperature validation discussed in Subsection 4.3.3.1. Validation of the moderator coefficient calculations is obtained by comparison with plant measurements at hot zero power conditions as shown in Table 4.3-13.

INSERT ①

Axial calculations are used to determine differential control rod worth curves (reactivity versus rod insertion) and axial power shapes during steady state and transient xenon conditions (flyspeck curve). Group constants and the radial buckling used in the axial calculation are obtained from the PANDA radial calculation, in which group constants in annular rings representing the various material regions in the X-Y plane are homogenized by flux-volume weighting.

INSERT ②

Validation of the spatial codes for calculating power distributions involves the use of incore and excore detectors and is discussed in Subsection 4.3.2.2.7.

Based on comparison with measured data it is estimated that the accuracy of current analytical methods is:

- ± 0.2 percent $\Delta\rho$ for Doppler defect
- ± 2 x 10^{-5}/°F for moderator coefficient
- ± 50 ppm for critical boron concentration with depletion
- ± 3 percent for power distributions
- ± 0.2 percent $\Delta\rho$ for rod bank worth
- ± 4 pcm/step for differential rod worth
- ± 0.5 pcm/ppm for boron worth
- ± 0.1 percent $\Delta\rho$ for moderator defect

INSERT 1 to 4.3.3.3

PALADON is used in two dimensional and three dimensional calculations. PALADON can be used in safety analysis calculations, ~~critical boron concentrations~~ and to determine critical boron concentrations, control rod worths, and reactivity coefficients.

~~INSERT 2~~

~~the three-dimensional TURTLE calculation or from the three-dimensional PALADON calculation~~

INSERT 2

Page 4.3-40
INSERT 2

the three-dimensional TURTLE calculation from which group constants are homogenized by flux-volume weighting.

4.3-28 Suich, J. E. and Honeck, H. C., "The HAMMER System, Hetergeneous Analysis by Multigroup Methods of Exponentials and Reactors," DP-1064, January, 1967.

4.3-29 Flatt, H. P. and Buller, D. C., "AIM-5, A Multigroup, One Dimensional Diffusion Equation Code," NAA-SR-4694, March, 1960.

4.3-~~30~~ 2 Moore, J. S., "Nuclear Design of Westinghouse Pressurized Water Reactors with Burnable Poison Rods," WCAP-9000-L, Revision 1 (Proprietary), July, 1969 and WCAP-7806, December, 1971.

4.3-33 Camden, T.M., et al., "PALADON - Westinghouse Nodal Computer Code," WCAP-9485A (Proprietary) and WCAP 9486A (Non-Proprietary), December 1979, and Supplement 1, September, 1981.

4.3-30 Nodvik, R.J., "Saxton Core II Fuel Performance Evaluation," WCAP-3385-56, Part II, "Evaluation of Mass Spectrometric and Radiochemical Analyses of Irradiated Saxton Plutonium Fuel," July, 1970.

4.3-31 Leamer, R.D., et al., "PuO_2-UO_2 Fueled Critical Experiments," WCAP-3726-1, July, 1967.

TABLE 4.3-1 (Continued)

REACTOR CORE DESCRIPTION

(First Cycle)

Diameter of Guide Thimbles (upper part), in.	0.450 I.D.
	0.482 O.D.
Diameter of Guide Thimbles (lower part), in.	0.397 I.D.
	0.429 O.D.
Diameter of Instrument Guide Thimbles, in.	0.450 I.D.
	0.482 O.D.
Fuel Rods	
Number	50,952
Outside Diameter, in.	0.374
Diametral Gap, in.	0.0065
Clad Thickness, in.	0.0225
Clad Material	Zircaloy-4
Fuel Pellets	
Material	UO_2 Sintered
Density (percent of Theoretical)	95
Fuel Enrichments, wt %	
Region 1	1.50
Region 2	2.20
Region 3	2.90
Diameter, in.	0.3225
Length, in.	0.530
Mass of UO_2 per Foot of Fuel Rod, lb/ft	~~0.364~~ .366
Rod Cluster Control Assemblies	
Neutron Absorber	Hafnium
Composition	~~100%~~ 95.3% Min.
Diameter, in.	0.341

30

TABLE 4.3-1 (Continued)

REACTOR CORE DESCRIPTION

(First Cycle)

Density, lb/in³	0.454 (min)	30
Cladding Material	Type 304, Cold Worked Stainless Steel	
Clad Thickness, in.	0.0185	30
Number of Clusters	57	30
Number of Absorber Rods per Cluster	24	
Burnable Poison Rods (First Core)		
Number	946	18
Material	Borosilicate Glass	
Clad Outside Diameter, in.	0.381	
Inner Tube, O.D., in.	0.1815	
Clad Material	Stainless Steel	
Inner Tube Material	Stainless Steel	
Boron Loading (w/o B_2O_3 in glass rod)	12.5	
Weight of Boron-10 per foot of rod, lb/ft	.000419	30
Initial Reactivity Worth, %$\Delta\rho$	4.65 (HFP), 4.65 (HZP) 3.40 (cold)	
Excess Reactivity		
Maximum Fuel Assembly k_∞ (Cold, Clean, Unborated Water)	1.39	
Maximum Core Reactivity (Cold, Zero Power, Beginning of Cycle)	1.22	

TABLE 4.3-2

NUCLEAR DESIGN PARAMETERS

(First Cycle)

Core Average Linear Power, kW/ft, including densification effects	5.20	
Total Heat Flux Hot Channel Factor, F_Q	2.50	
Nuclear Enthalpy Rise Hot Channel Factor, $F^N_{\Delta H}$	1.52	
Reactivity Coefficients+	Design Limits	Best Estimate
Doppler-only Power, Upper Curve Coefficients, pcm/°F++	-19.4 to -12.6	~~-13~~ -15.5 to ~~-11~~ -11.5
(See Figure 15.0-5), Lower Curve	-10.2 to -6.7	~~-13~~ -12.5 to -9 |3
Doppler Temperature Coefficient pcm/°F++	-2.9 to -1.1	-2.5 to ~~-1.9~~ -1.8
Moderator Temperature Coefficient, pcm/°F++	0 to -40	-6. to -30.0
Boron Coefficient, pcm/ppm++	-16 to -7	-14. to -9
Rodded Moderator Density Coefficient, pcm/gm/cc++	$\leq 0.43 \times 10^5$	$\leq 0.34 \times 10^5$

+Uncertainties are given in Section 4.3.3.3

ATTACHMENT 1
ST-HL-AE-1432
PAGE 35 OF 54

TABLE 4.3-2 (Continued)

NUCLEAR DESIGN PARAMETERS

(First Cycle)

Radial Factor (BOL to EOL)	
Unrodded	1.41 ~~1.39~~ to 1.28
D bank	1.50 to 1.45
D + C	1.60 to 1.45
D + C + B	1.80 to 1.55
Boron Concentrations, BOL, ppm	
Zero Power, k_{eff} = 0.99, Cold, Rod Cluster Control Assemblies Out, clean	1080
Zero Power, k_{eff} = 0.99, Hot, Rod Cluster Control Assemblies Out, clean	1030
Design Basis Refueling Boron Concentration	2500
Zero Power, $k_{eff} \leq 0.95$, Cold, Rod Cluster Control Assemblies In, clean	910
Zero Power, k_{eff} = 1.00, Hot, Rod Cluster Control Assemblies Out, clean	930
Full Power, No Xenon, k_{eff} = 1.0, Hot, Rod Cluster Control Assemblies Out	835
Zero Power, K_{eff} = .99, Cold, Rod Cluster Control Assemblies in Less Most Reactive Rod Stuck in Full Out Position	730

TABLE 4.3-4

COMPARISON OF REACTIVITY REQUIREMENTS

	End of Life (Equilibrium Cycle) 3800 MWt 168 inch fuel	End of Life (Equilibrium Cycle) 3411 MWt 144 inch fuel	
1. Control Requirements			
a. Fuel Temperature (Doppler), $\% \Delta\rho$ + Moderator Temperature, $\% \Delta\rho$ + Void, $\% \Delta\rho$ + Rod Insertion Allowance, $\% \Delta\rho$	2.95	2.94	
b. Redistribution, $\% \Delta\rho$	1.20	0.85	
2. Total Control, $\% \Delta\rho$	4.15	3.79	
3. Estimated Rod Cluster Control Assembly Worth			
a. Number of Control Rod Clusters	57	53	30
b. Worth of all assemblies, $\% \Delta\rho$	8.50	7.30	30
c. Worth of all but one Assembly (highest worth), $\% \Delta\rho$	6.90	6.20	
4. Estimated Rod Cluster Control Assembly credit with 10 percent adjustment to accommodate uncertainties (3c - 10 percent), $\% \Delta\rho$	6.20	5.58	
5. Shutdown Margin Available (4-2), $\% \Delta\rho$	2.05 ~~2.08~~ [a]	1.79 [b]	

[a] The design basis minimum shutdown is 1.75% $\Delta\rho$
[b] The design basis minimum shutdown is 1.60% $\Delta\rho$

ATTACHMENT 1
ST-HL-AE-1432
PAGE 38 OF 54

TABLE 4.3-6

BENCHMARK CRITICAL EXPERIMENTS

Description of Experiments*	Number of Experiments	LEOPARD k_{eff} Using Experimental Bucklings
UO_2		
Al clad	14	1.0012
SS clad	19	0.9963
Borated H_2O	7	0.9989
Subtotal	40	0.9985
U-Metal		
Al clad	41	0.9995
Unclad	20	0.9990
Subtotal	61	0.9993
Total	101	0.9990

* Reported in Reference [4.3-~~12~~3] 14

TABLE 4.3-10

SAXTON CORE II ISOTOPICS

ROD MY, AXIAL ZONE 6

Atom Ratio	Measured*	2σ Precision (%)	LEOPARD Calculation
U-234/U	4.65×10^{-5}	±29	4.60×10^{-5}
U-235/U	5.74×10^{-3}	±0.9	5.73×10^{-3}
U-236/U	3.55×10^{-4}	±5.6	3.74×10^{-4}
U-238/U	0.99386	±0.01	0.99385
Pu-238/Pu	1.32×10^{-3}	±2.3	1.222×10^{-3}
Pu-239/Pu	0.73971	±0.03	0.74497
Pu-240/Pu	0.19302	±0.2	0.19102
Pu-241/Pu	6.014×10^{-2}	±0.3	5.74×10^{-2}
Pu-242/Pu	5.81×10^{-3}	±0.9	5.38×10^{-3}
Pu/U**	5.938×10^{-2}	±0.7	5.970×10^{-2}
Np-237/U-238	1.14×10^{-4}	±15	0.86×10^{-4}
Am-241/Pu-239	1.23×10^{-2}	±15	1.08×10^{-2}
Cm-242/Pu-239	1.05×10^{-4}	±10	1.11×10^{-4}
Cm-244/Pu-239	1.09×10^{-4}	±20	0.98×10^{-4}

* Reported in Reference [4.3-~~29~~] 30

** Weight ratio

ATTACHMENT 1
ST-HL-AE-1432
PAGE 40 OF 54

TABLE 4.3-12

COMPARISON OF MEASURED AND CALCULATED ROD WORTH

2-Loop Plant, 121 Assemblies, 10 foot core	Measured (pcm)	Calculated (pcm)
Group B	1885	1893
Group A	1530	1649
Shutdown Group	3050	2917
ESADA-Critical*, 0.69" Pitch, 2 w/o PuO_2, 8% Pu^{240}, 9 Control Rods		
6.21" rod separation	2250	2250
2.07" rod separation	4220	4160
1.38" rod separation	4010	4010

* Reported in Reference [4.3-~~30~~ 31]

19996-1

REPLACE WITH
NEW FIGURE

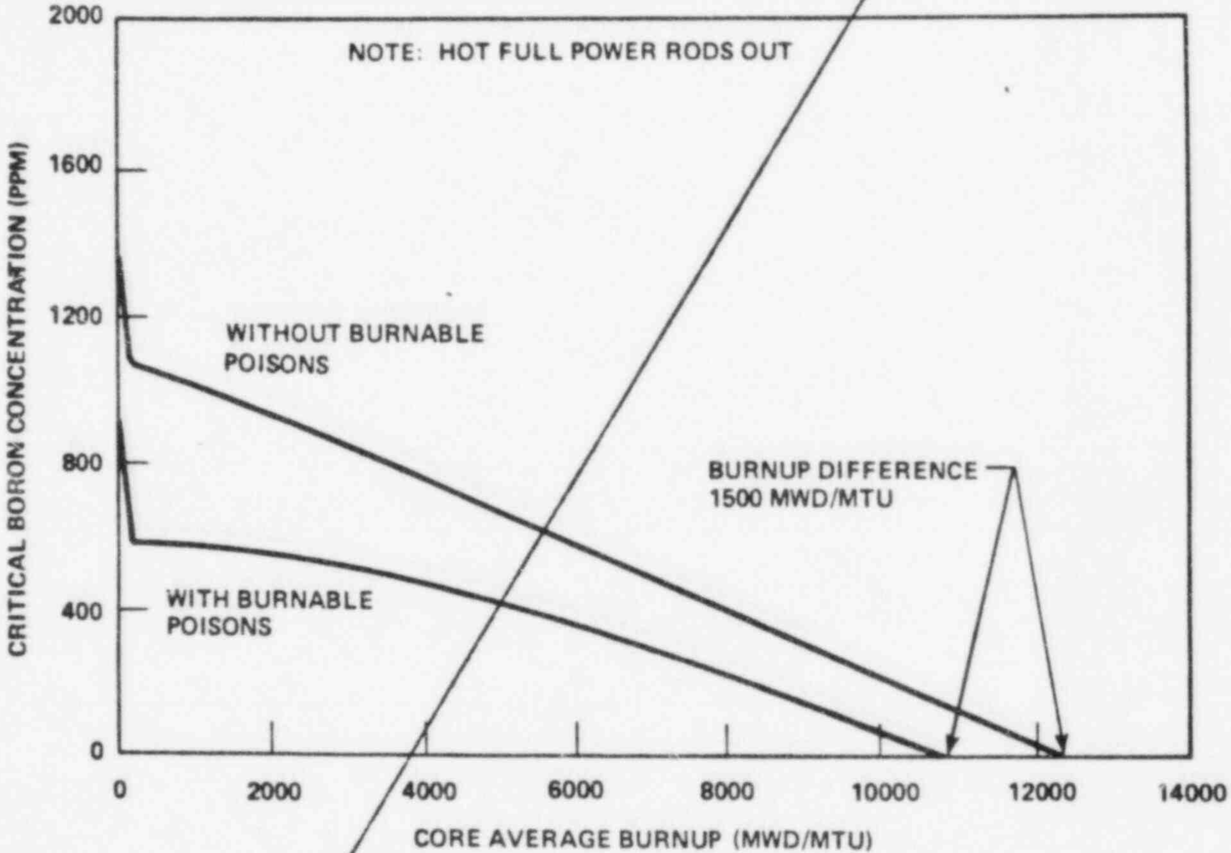

Amendment 26

SOUTH TEXAS PROJECT
UNITS 1 & 2

Boron Concentration versus First Cycle Burn-up With and Without Burnable Poison Rods

Figure 4.3-3

ATTACHMENT 1
ST-HL-AE-1432
PAGE 42 OF 54

19996 1

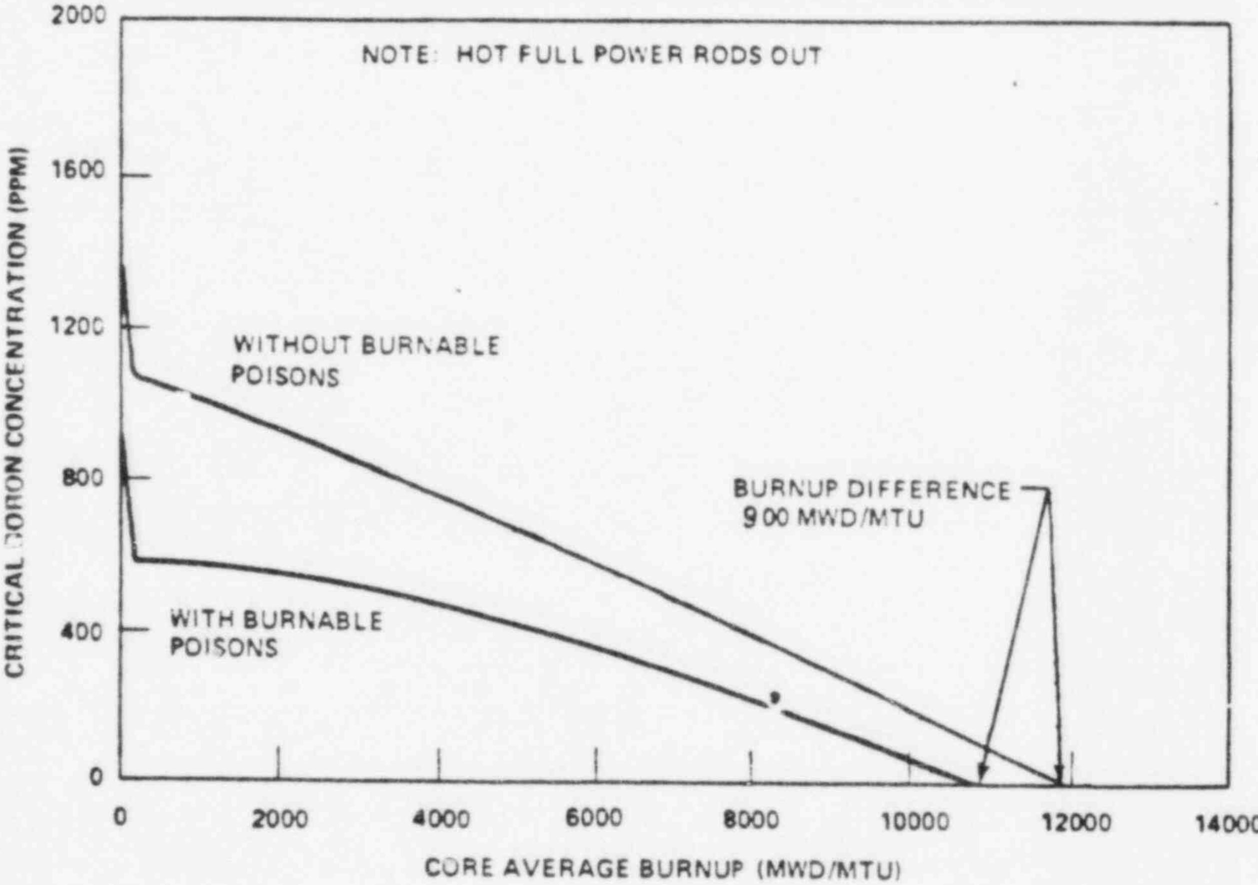

Amendment 26

SOUTH TEXAS PROJECT UNITS 1 & 2

Boron Concentration versus First Cycle Burnup With and Without Burnable Poison Rods

Figure 4.3-3

ATTACHMENT 1
ST-HL-AE- 1432
PAGE 43 OF 54

12,373-10

REPLACE WITH NEW FIGURE

180°

90° / 270°

	R	P	N	M	L	K	J	H	G	F	E	D	C	B	A
1						4		4		4					
2					9		24		1S 23		9				
3			3	24		4		4S 8		4		24	3		
4			24		12		8		8		12		24		
5		9		12		8		8		8		12		9	
6	4		4		8		8		8		8		4		4
7		24		8		8		12		8		8		24	
8	4		8		8		12		12		8		8		4
9		24		8		8		12		8		8		24	
10	4		4		8		8		8		8		4		4
11		9		12		8		8		8		12		9	
12			24		12		8		8		12		24		
13			3	24		4		4S 8		4		24	3		
14					9		24		1S 23		9				
15						4		4		4					

0°

NUMBER INDICATES NUMBER OF BURNABLE POISON RODS
S - INDICATES SOURCE ROD

946 BP RODS
12.5 W/O B_2O_3

Amendment 18, 5/1/81

SOUTH TEXAS PROJECT UNITS 1 & 2

Figure 4.3-5.

Burnable Poison Loading Pattern

180°

	R	P	N	M	L	K	J	H	G	F	E	D	C	B	A
1						4		4		4					
2					9		24		1S 23		9				
3			3	24		4		8		4		24	3		
4			24		12		8		8		12		24		
5		9		12		8	4S	8		8		12		9	
6	4		4		8		8		8		8		4		4
7		24		8		8		12		8		8		24	
8	4		8		8		12		12		8		8		4
9		24		8		8		12		8		8		24	
10	4		4		8		8		8		8		4		4
11		9		12		8		8	4S	8		12		9	
12			24		12		8		8		12		24		
13			3	24		4		8		4		24	3		
14					9		24		1S 23		9				
15						4		4		4					

90° (left) 270° (right)

0°

NUMBER INDICATES NUMBER OF BURNABLE POISON RODS
S - INDICATES SOURCE ROD

946 BP RODS
12.5 W/O B_2O_3

~~Amendment 18, 5/1/81~~

SOUTH TEXAS PROJECT
UNITS 1 & 2

Figure 4.3-5.

Burnable Poison Loading Pattern

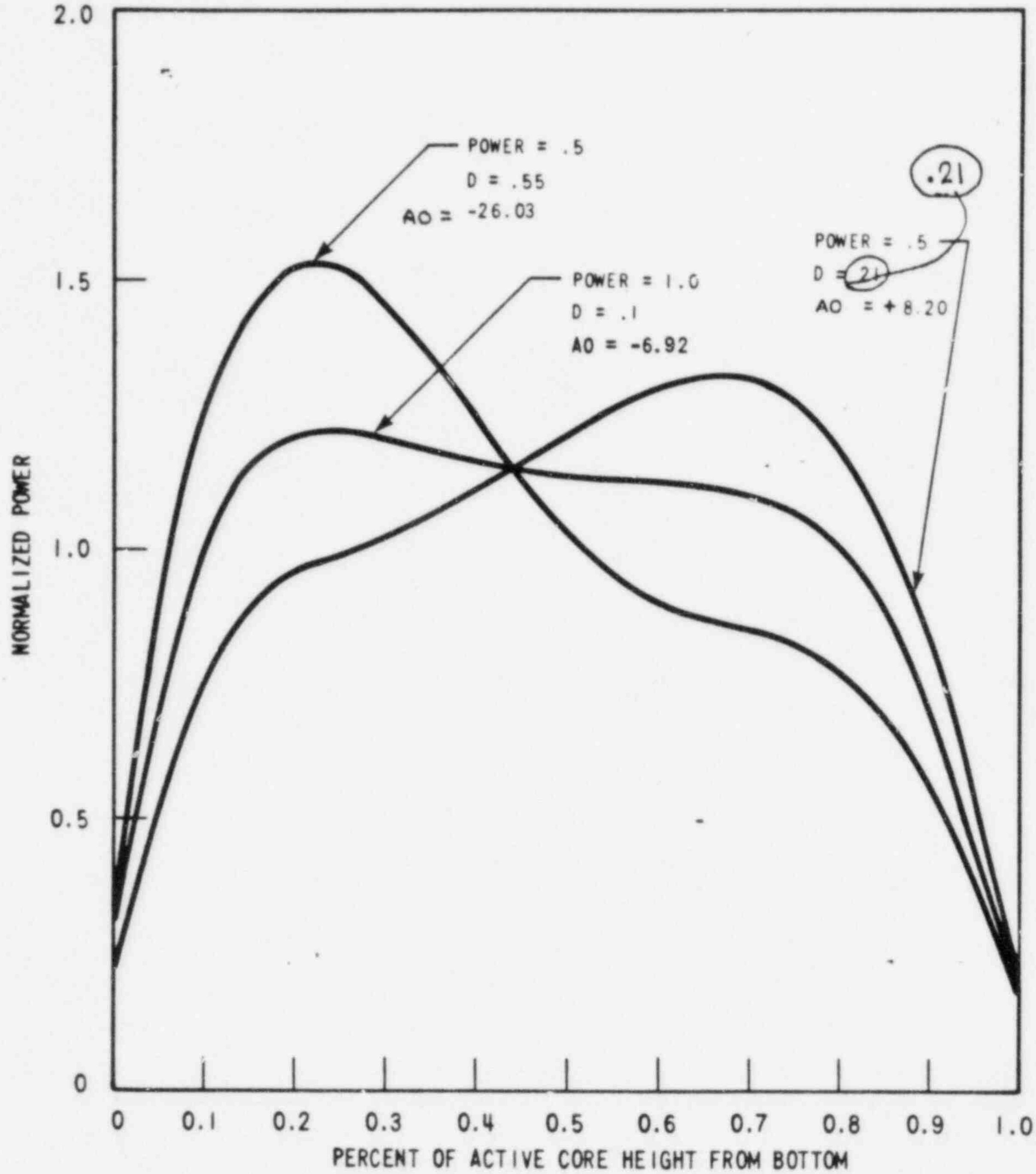

LEGEND:
D = FRACTIONAL INSERTION OF D BANK
AO = AXIAL OFFSET

Amendment 1, 7/19/78

SOUTH TEXAS PROJECT
UNITS 1 & 2

Typical Axial Power Shapes Occuring at Middle of Life
Figure 4.3-15.

$$q''_{DNB,N} = \frac{q''_{DNB,\,EU}}{F} \qquad (4.4\text{-}5)$$

and $q''_{DNB,EU}$ is the uniform DNB heat flux as predicted by the W-3 DNB correlation, Reference 4.4-10 all flow cell walls are heated.

F is the flux shape factor to account for nonuniform axial heat flux distributions, Reference 4.4-10, with the "C" term modified as in Reference 4.4-3.

F'_S is the modified spacer factor defined by Equation (4.4-1) in Subsection 4.4.2.2.1 and using an axial grid spacing coefficient, $K_S = 0.059$, and a thermal diffusion coefficient (TDC) of 0.059, based on the 22 in. grid spacing data previously described. Since the actual grid spacing is 19.8 in., the modified spacer factor is conservative since the DNB performance was found to improve and TDC increases as axial grid spacing is decreased, References 4.4-8 and 4.4-12. The TDC value for 20 in. grid spacing (approximately the same spacing as this design) is 0.061. 18

q''_{loc} is the actual local heat flux.

The DNB heat flux ratio as applied to this design when a cold wall is present is:

$$DNBR = \frac{q''_{DNB,N,CW} \times F'_S}{q''_{loc}} \qquad (4.4\text{-}6)$$

where:

$$q''_{DNB,N,CW} = \frac{q''_{DNB,EU,Dh} \times CWF}{F} \qquad (4.4\text{-}7)$$

where:

$q''_{DNB,EU,Dh}$ is the uniform DNB heat flux as predicted by the W-3 cold wall DNB correlation, Reference 4.4-3, when not all flow cell walls are heated (thimble cold wall cell).

$$CWF^{[4.4-3]} = 1.0 - Ru\,[13.76 - 1.372e^{1.78x} - 4.732\left(\frac{G}{10^6}\right)^{0.0535} - 0.0619\left(\frac{P}{1000}\right)^{0.14} - 8.509Dh^{0.107}] \qquad (4.4\text{-}8)$$

and $Ru = 1 - De/Dh$

F'_S defined by Equation (4.4-1) in Subsection 4.4.2.2.1 is the same as used for typical cell.

Values of minimum DNB provided in Table 4.4-1 and 4.4-2 are the limiting value obtained by applying the above two definitions of DNBR to the appropriate cell (typical cell with all walls heated, or a thimble cold wall cell with a partial heated wall condition).

The procedures used in the evaluation of DNB margin for this application show that the calculated minimum DNBR for the peak rod or rods in the core will be above 1.30 during Class I and II incidents, even when all the engineering hot 18

ATTACHMENT 1
ST-HL-AE-1432
PAGE 47 OF 54

1. Pellet diameter, density and enrichment |18

Design values employed in the THINC analysis related to the above fabrication variations are based on applicable limiting tolerances such that these design values are met for 95 percent of the limiting channels at a 95 percent confidence level. Measured manufacturing data on Westinghouse 17 x 17 fuel show the tolerances used in this evaluation are conservative. The |18 effect of variations in pellet diameter, enrichment and density is employed in the THINC analysis as a direct multiplier on the hot channel enthalpy |18 rise.

2. Inlet Flow Maldistribution

The consideration of inlet flow maldistribution in core thermal performances is discussed in Section 4.4.4.2.2. A design basis of 5 percent reduction in coolant flow to the hot assembly is used in the THINC-IV analysis.

3. Flow Redistribution

The flow redistribution accounts for the reduction in flow in the hot channel resulting from the high flow resistance in the channel due to the local or bulk boiling. The effect of the non-uniform power distribution is inherently considered in the THINC analysis for every operating condition which is evaluated.

4. Flow Mixing

The subchannel mixing model incorporated in the THINC Code and used in reactor design is based on experimental data (4.4-17) discussed in Section 4.4.4.5.1. The mixing vanes incorporated in the spacer grid design induce additional flow mixing between the various flow channels in a fuel assembly as well as between adjacent assemblies. This mixing reduces the enthalpy rise in the hot channel resulting from local power peaking or unfavorable mechanical tolerances.

4.4.2.2.5 <u>Effects of Rod Bow on DNBR:</u> The phenomenon of fuel rod bowing, as described in Reference 4.4-84, must be accounted for in the DNBR safety analysis of Condition I and Condition II events for each plant application. Applicable generic credits for margin resulting from retained conservatism in the evaluation of DNBR and/or margin obtained from measured plant operating parameters (such as $F^N_{\Delta H}$ or core flow), which are less limiting than those required by the plant safety analysis, can be used to offset the effect of rod bow. 43

The safety analysis for South Texas cores maintained sufficient margin (3.3 percent) to accommodate full and low flow DNBR penalties identified in Reference 4.4-85 with the incorporation of the L^2/I scaling factor (I = fuel rod bending moment of inertia, L = span length) to account for 17X17 XL span lengths. A design limit DNBR of 1.30 vs. 1.28, a grid spacing coefficient (K_S) of .059 vs. .066, and a thermal diffusion coefficient (TDC) of .059 vs. .051 are examples of conservatism utilized in the safety analysis.

The maximum rod bow penalties accounted for in the design safety analysis are based on an assembly average burnup of 33,000 MWd/MTU. At burnups

(used for modified spacer factor, F_S' only) greater than 33,000 MWd/MTU, credit is taken for the effect of $F_{\Delta H}^{N}$ burndown, due to the decrease in fissionable isotopes and the buildup of fission product inventory, and no additional rod bow penalty is required. 43

4.4.2.3 Linear Heat Generation Rate. The core average and maximum Linear Powers are given in Table 4.4-1. The method of determining the maximum Linear Powers is given in Section 4.3.2.2.

4.4.2.4 Void Fraction Distribution. The calculated core average and the hot subchannel maximum and average void fractions are presented in Table 4.4-3 for operation at full power with design hot channel factors. The void fraction distribution in the core at various radial and axial locations is presented in Reference (4.4-18). The void models used in the THINC-IV computer code are described in Section 4.4.2.7.3. Normalized core flow and enthalpy rise distributions are shown on Figures 4.4-5 through 4.4-7.

4.4.2.5 Core Coolant Flow Distribution. Assembly average coolant mass velocity and enthalpy at various radial and axial core locations are given below. Coolant enthalpy rise and flow distributions are shown for the 1/3 core height elevation on Figure 4.4-5, and 2/3 core height elevation on Figure 4.4-6 and at the core exit on Figure 4.4-7. These distributions are for the full power conditions as given in Table 4.4-1 and for the radial power density distribution shown on Figure 4.3-7. The THINC Code analysis for this case utilized a uniform core inlet enthalpy and inlet flow distribution. No orificing is employed in the reactor design.

4.4.2.6 Core Pressure Drops and Hydraulic Loads.

4.4.2.6.1 Core Pressure Drops: The analytical model and experimental data used to calculate the pressure drops shown in Table 4.4-1 are described in Section 4.4.2.7. The core pressure drop includes the fuel assembly, lower core plate, and upper core plate pressure drops. The full power operation pressure drop values shown in Table 4.4-1 are the unrecoverable pressure drops across the vessel, including the inlet and outlet nozzles, and across the core. These pressure drops are based on the best estimate flow for actual plant operating conditions as described in Section 5.1.1. This section also defines and describes the thermal design flow (minimum flow) which is the basis for reactor core thermal performance and the mechanical design flow (maximum flow) which is used in the mechanical design of the reactor vessel internals and fuel assemblies. Since the best estimate flow is that flow which is most likely to exist in an operating plant, the calculated core pressure drops in Table 4.4-1 are based on this best estimate flow rather than the thermal design flow.

Uncertainties associated with the core pressure drop values are discussed in Section 4.4.2.9.2.

4.4.2.6.2 Hydraulic Loads: The fuel assembly hold down springs, Figure 4.2-2, are designed to keep the fuel assemblies in contact with the lower core plate under all Condition I and II events with the exception of the turbine overspeed transient associated with a loss of external load. The hold down springs are designed to tolerate the possibility of an over deflection associated with fuel assembly liftoff for this case and provide contact between the fuel assembly and the lower core plate following this 18

ATTACHMENT 1
ST-HL-AE-1432
PAGE 49 OF 54

6. Line lengths and sizes for the Safety Injection System (SIS) are determined so as to guarantee a total system resistance which will provide, as a minimum, the fluid delivery rates assumed in the safety analyses described in Chapter 15.

7. The parameters for components of the RCS are presented in Section 5.4, component and subsystem design.

8. The steady state pressure drops and temperature distributions through the RCS are presented in Table 5.1-1.

4.4.3.2 Operating Restrictions on Pumps. The minimum net positive suction head (NPSH) and minimum seal injection flow rate must be established before operating the reactor coolant pumps. With the minimum 6 gpm labyrinth seal injection flow rate established, the operator will have to verify that the system pressure satisfies NPSH requirements.

4.4.3.3 Power-Flow Operating Map (BWR). Not applicable to STP.

4.4.3.4 Temperature-Power Operating Map. The relationship between RCS temperature and power is shown on Figure 4.4-21.

The effects of reduced core flow due to inoperative pumps is discussed in Sections 5.4.1, 15.2.5, and 15.3.4. Natural circulation capability of the system is shown in Table 15.2-2.

4.4.3.5 Load Following Characteristics. The RCS is designed on the basis of steady state operation at full power heat load. The reactor coolant pumps utilize constant speed drives as described in Section 5.4 and the reactor power is controlled to maintain average coolant temperature at a value which is a linear function of load, as described in Section 7.7.

4.4.3.6 Thermal and Hydraulic Characteristics Summary Table. The thermal and hydraulic characteristics are given in Tables 4.3-1, 4.4-1, and ~~and 4.4-2.~~

4.4.4 Evaluation

4.4.4.1 Critical Heat Flux. The critical heat flux correlation utilized in the core thermal analysis is discussed in Section 4.4.2.

4.4.4.2 Core Hydraulics.

4.4.4.2.1 Flow Paths Considered in Core Pressure Drop and Thermal Design: The following flow paths or core bypass flow are considered:

1. Flow through the spray nozzles into the upper head for head cooling purposes.

2. Flow entering into the rod cluster control guide thimbles to cool the control rods.

The way in which $F^N_{\Delta H}$ is used in the DNB calculation is important. The location of minimum DNBR depends on the axial profile and the value of DNBR depends on the enthalpy rise to that point. Basically, the maximum value of the rod integral is used to identify the most likely rod for minimum DNBR. An axial power profile is obtained which when normalized to the design value of $F^N_{\Delta H}$, recreates the axial heat flux along the limiting rod. The surrounding rods are assumed to have the same axial profile with rod average powers which are typical distributions found in hot assemblies. In this manner, worst case axial profiles can be combined with worst case radial distributions for reference DNB calculations.

It should be noted again that $F^N_{\Delta H}$ is an integral and is used as such in DNB calculations. Local heat fluxes are obtained by using hot channel and adjacent channel explicit power shapes which take into account variations in horizontal power shapes throughout the core. The sensitivity of the THINC-IV analysis to radial power shapes is discussed in Reference 4.4-18.

For operation at a fraction P of full power, the design $F^N_{\Delta H}$ used is given by:

$$F^N_{\Delta H} = 1.52\ [1 + 0.3\ (1-P)] \qquad (4.4\text{-}19)$$

The permitted relaxation of $F^N_{\Delta H}$ is included in the DNB protection setpoints and allows radial power shape changes with rod insertion to the insertion limits [4.4-66], thus allowing greater flexibility in the nuclear design.

4.4.4.3.2 <u>Axial Heat Flux Distributions</u>: As discussed in Subsection 4.3.2.2, the axial heat flux distribution can vary as a result of rod motion, power change, or due to spatial xenon transients which may occur in the axial direction. Consequently it is necessary to measure the axial power imbalance by means of the excore nuclear detectors (as discussed in Subsection 4.3.2.2.7) and protect the core from excessive axial power imbalance. The reactor trip system provides automatic reduction of the trip setpoint in the overtemperature ΔT channels on excessive axial power imbalance; that is, when an extremely large axial offset corresponds to an axial shape which could lead to a DNBR which is less than that calculated for the reference DNB design axial shape.

Replace with Insert 4.4-1

The normal reference DNB design axial shape is either a chopped cosine shap a peak to average value of 1.55 or a skewed-to-the-top shape, depending upo which is more conservative in each application. The reference DNB axial sh used in establishing core DNB limits (i.e., overtemperature ΔT protection s setpoints) and Condition II accidents ~~is a~~ chopped cosine shape with a peak to average value ~~slightly greater than 1.55~~. Exceptions to this are loss of flow with pump(s) coasting down freely, a single dropped full length control rod, and statically misaligned full length control rod which are initiated from normal full power operation. Since there are fewer axial power shapes which give DNBR's less than this shape as compared to the reference DNB design axial shape, greater axial power imbalanc can be allowed and, thus, increases plant operating flexibility.

INSERT 4.4-1

The normal reference DNB design axial shape is either a chopped cosine shape with a peak to average value of 1.55 or a skewed-to-the-top shape, depending upon which is more conservative in each application. The reference DNB axial shape used in establishing core DNB limits (i.e., overtemperature ΔT protection system setpoints) and Condition II accidents for the South Texas plants is a chopped cosine shape with a peak to average value of 1.61. With respect to minimum DNBR, this axial shape bounds all of the shapes which could occur during power operation including overpower conditions as generated for the nuclear design (refer to Section 4.3.2.2.6). Accidents which are initiated from normal full power operation including loss of flow with pump(s) coasting down freely, a single dropped control rod, and a statically misaligned control rod are analyzed with a 1.55 chopped cosine axial shape because this shape bounds all of the possible shapes which could occur at normal full power operating conditions.

To determine the penalty to be taken in protection set points for extreme values of flux difference, ~~this~~ the reference shape (1.61 chopped cosine) is supplemented by other axial shapes skewed to the bottom and top of the core. The course of those accidents in which DNB is a concern is analyzed in Chapter 15 assuming that the protection set points have been set on the basis of these shapes. In many cases the axial power distribution in the hot channel changes throughout the course of the accident due to rod motion, coolant temperature and power level changes.

The initial conditions for the accidents for which DNB protection is required are assumed to be those permissible within the constant axial offset control strategy for the load maneuvers described in Reference 4.4-67. In the case of the loss of flow accident the hot channel heat flux profile is very similar to the power density profile in normal operation preceding the accident. It is therefore possible to illustrate the calculated minimum DNB ratio for conditions representative of the loss of flow accident as a function of the flux difference initially in the core. A plot of this type is provided on Figure 4.4-10 for first core initial conditions. As noted on this figure, all power shapes were evaluated with a full power radial peaking factor ($F^N_{\Delta H}$) of 1.52. The radial contribution to the hot rod power shape is conservative both for the initial condition and for the condition at the time of minimum DNBR during the loss of flow transient. Also shown is the minimum DNBR calculated for the reference normal full power shape (1.55 Chopped cosine) at the same conditions.

4.4.4.4 <u>Core Thermal Response</u>. A general summary of the steady-state thermal-hydraulic design parameters including thermal output, flow rates, etc., is provided in Table 4.4-1.

As stated in Section 4.4-1, the design bases of the application are to prevent DNB and to prevent fuel melting for Condition I and II events. The protective systems described in Chapter 7 are designed to meet these bases. The response of the core to Condition II transients is given in Chapter 15.

4.4.4.5 <u>Analytical Techniques</u>.

4.4.4.5.1 <u>Core Analysis</u>: The objective of reactor core thermal design is to determine the maximum heat removal capability in all flow subchannels and to show that the core safety limits (as will be presented in the Technical Specifications) are not exceeded while compounding engineering and nuclear effects. The thermal design considers local variations in dimensions, power generation, flow redistribution, and mixing. THINC-IV is a realistic three-dimensional matrix model which has been developed to account for hydraulic and nuclear effects on the enthalpy rise in the core. (References 4.4-18 and 4.4-49) The behavior of the hot assembly is determined by superimposing the power distribution among the assemblies upon the inlet flow distribution while allowing for flow mixing and flow distribution between assemblies. The average flow and enthalpy in the hottest assembly is obtained from the core-wide, assembly by assembly analysis. The local variations in power, fuel rod and pellet fabrication, and mixing within the hottest assembly are then superimposed on the average conditions of the hottest assembly in order to determine the conditions in the hot channel.

4.4-71. Weismann, J., Wenzel, A. H., Tong, L.S., Fitzsimmons, D., Thorne, W. and Batch, J., "Experimental Determination of the Departure from Nucleate Boiling in Large Rod Bundles at high Pressures," Chem. Eng. Prog. Symp. Ser. 64, No. 82, 114-125 (1968).

4.4-72. Boure, J. A., Bergles, A. E. and Tong, L.S., "Review of Two-Phase Flow Instability," Nucl. Engr. Design 25 (1973) p. 165-192.

4.4-73. Lahey, R. T., and Moody, F. J., "The Thermal Hydraulics of a Boiling Water Reactor," American Nuclear Society, 1977.

4.4-74. Saha P., Ishii, M., and Zuber N., "An Experimental Investigation of the Thermally Induced Flow Oscillations in Two-Phase Systems," J. of Heat Transfer, Nov. 1976, pp. 616-622.

4.4-75. Summer, ~~Virgin C.~~ Virgil C, FSAR, Docket #50-395. 6

4.4-76. Byron/Braidwood FSAR, Docket #50-456.

4.4-77. Comanche Peak FSAR, Docket #50-445.

4.4-78. Kakac, S., Veziroglu, T. N., Akyuzlu, K., Berkol, O., "Sustained and Tranient Boiling Flow Instabilities in a Cross-Connected Four-Parallel-Channel Upflow System," Proc. of 5th International Heat Transfer Conference, Tokyo, Sept. 3-7, 1974.

4.4-79. Kao, H. S., Morgan, C. D., and Parker, W. B., "Prediction of Flow Oscillation in Reactor Core Channel," Trans. ANS, Vol. 16, 1973, pp. 212-213.

4.4-80. (This reference has beeen deleted.) 7

4.4-81. Ohtsubo, A., and Uruwashi, S., "Stagnant Fluid due to Local Flow Blockage," J. Nucl. Sci. Technol., 9,, No. 7, 433-434, (1972).

4.4-82. Basamer, P., Kirsch, D. and Schultheiss, G. F., "Investigation of the Flow Pattern in the Recirculation Zone Downstream of Local Coolant Blockages in Pin Bundles," Atomwirtschaft, 17, No. 8, 416-417, (1972). (In German).

4.4-83. Burke, T. M., Meyer, C. E. and Shefcheck J., "Analysis of Data from the Zion (Unit 1) THINC Verification Test," WCAP-8453 (Proprietary), December, 1974 and WCAP-8454, December, 1974.

4.4-84. Skaritka, J., (Ed.), "Fuel Rod Bow Evaluation," WCAP-8691, Rev.1 (Proprietary) July 1979.

4.4-85. "Partial Response to Request Number 1 for Additional Information on WCAP-8691, Revision 1" Letter, E. P. Rahe, Jr., (Westinghouse) to J. R. Miller (NRC), NS-EPR-2515, dated October 9, 1981; "Remaining Response to Request Number 1 for Additional Information on WCAP-8691, Revision 1" Letter, E. P. Rahe, Jr., (Westinghouse) to J. R. Miller (NRC), NS-EPR-2572, dated March 16, 1982. 43

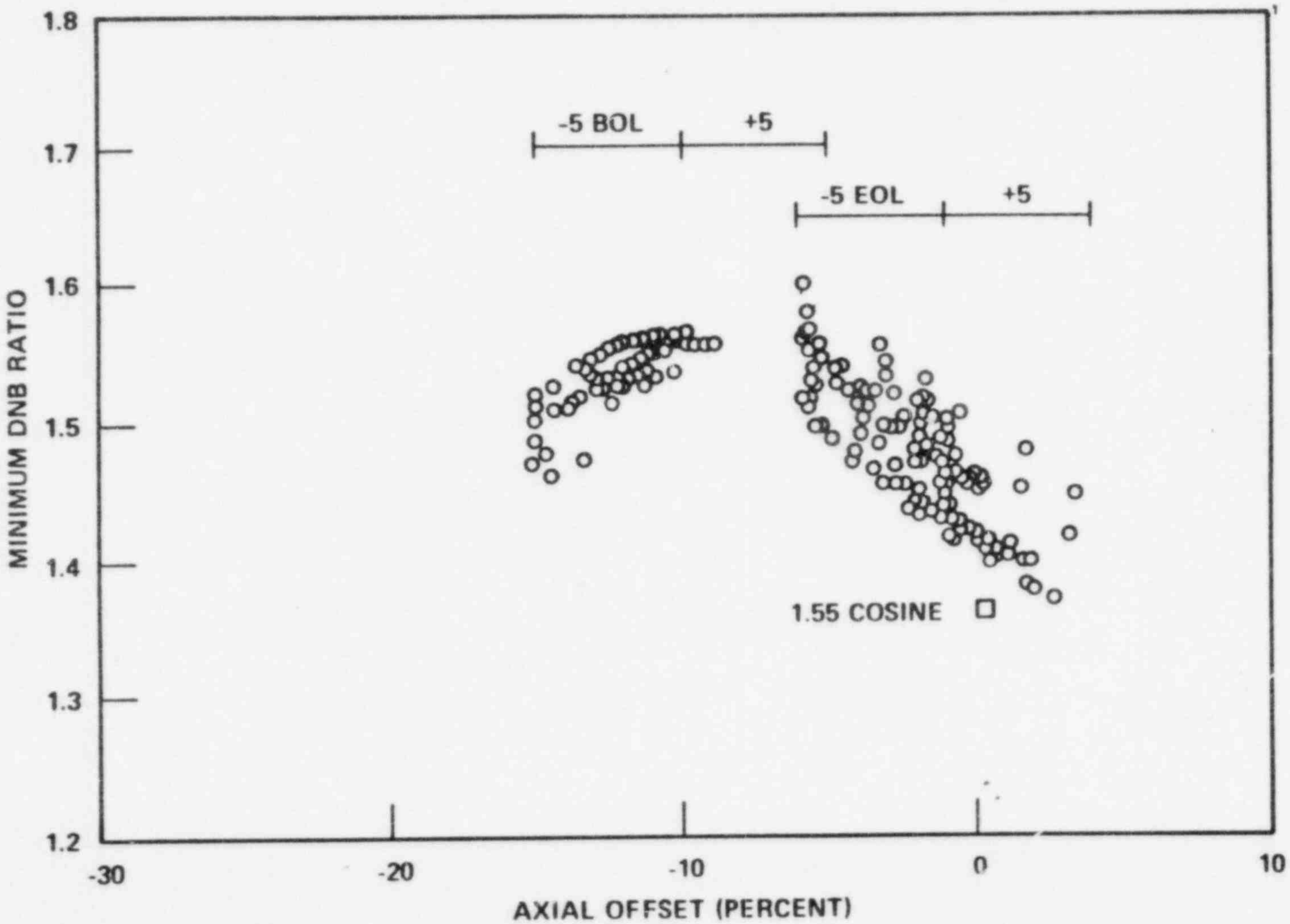

15,591-11

SOUTH TEXAS PROJECT
UNITS 1 & 2

Amendment 18, 5/1/81

Figure 4.4-10.
100% Power Shapes Evaluated at Conditions Representative of Loss of Flow all Shapes Evaluated with $F_{\Delta H}^{N}$ = ~~1.65~~ ($F_{\Delta H}^{N}$ = 1.52)